SOME STUDIES ON GOLD-DOPED GERMANIUM

by

ABDUS SATTAR SYED
B.Sc.(Hons), University of Dacca, 1953
M.Sc. University of Dacca, 1954

A THESIS SUBMITTED IN PARTIAL FULFILMENT OF
THE REQUIREMENTS FOR THE DEGREE OF

DOCTOR OF PHILOSOPHY

in the Department

of

Physics

We accept this thesis as conforming to the
required standard

THE UNIVERSITY OF BRITISH COLUMBIA
August, 1964

In presenting this thesis in partial fulfilment of the requirements for an advanced degree at the University of British Columbia, I agree that the Library shall make it freely available for reference and study. I further agree that permission for extensive copying of this thesis for scholarly purposes may be granted by the Head of my Department or by his representatives. It is understood that copying or publication of this thesis for financial gain shall not be allowed without my written permission.

Department of Physics

The University of British Columbia,
Vancouver 8, Canada

Date September 30, 1964

The University of British Columbia

FACULTY OF GRADUATE STUDIES

PROGRAMME OF THE

FINAL ORAL EXAMINATION

FOR THE DEGREE OF

DOCTOR OF PHILOSOPHY

of

ABDUS SATTAR SYED

B.Sc. (Hons.), University of Dacca, Pakistan, 1953
M.Sc., University of Dacca, Pakistan, 1954

MONDAY, SEPTEMBER 28, 1964, AT 4:00 P.M.
ROOM 301, HENNINGS BUILDING (Physics)

COMMITTEE IN CHARGE

Chairman: I. McT. Cowan

R. Barrie
J. W. Bichard
A. V. Bree
R. E. Burgess
C. F. Schwerdtfeger
E. Teghtsoonian

External Examiner: H.Y. Fan
Duncan Professor of Physics
Purdue University

SOME STUDIES ON GOLD-DOPED GERMANIUM

ABSTRACT

Tyler used Hall coefficient measurements to evaluate the gold acceptor concentration in germanium crystallized from a germanium-gold melt at a temperature between the melting point of pure germanium and 17°K below this temperature. The present study reports the results of similar measurements in the temperature range of growth from 12° to 80°K below the melting point of germanium. A crystal grower was designed and constructed for growing the monocrystals of gold-doped germanium.

It was found that the ⟨100⟩ direction was the most favorable direction for eliminating dendritic growth on gold-rich phase crystallized as inclusions. The phenomenon of retrograde solubility was observed. The maximum solubility ($\sim 2.8 \times 10^{16}$ gold acceptor atoms per c.c.) occurred at about 30°K below the melting point of pure germanium.

Infra-red absorption in gold-doped germanium was studied between 4.2° and 298°K over the energy range from 0.08 to 0.6 e.v. The magnitudes of the absorption cross-sections for the specimens containing about 3.5×10^{15} and 1.2×10^{15} gold acceptor atoms per c.c. were in close agreement with the data of Johnson and Levinstein. The cross-section of absorption near the band gap of germanium for the heavily gold-doped germanium ($> 10^{16}$ gold acceptor atoms per c.c.) is about the same as in the case of lightly doped specimens. Whereas in the case of lightly doped specimens, however, the cross-section of absorption drops sharply to negligible values as the energy of the incident photon decreases, the cross-section of absorption for the heavily doped specimen remains very high. The excess absorption is found to remain substantially the same when measurements are extended to the energy range between 0.032 and 0.044 e.v.

At 298°K, the absorption of infra-red radiation in gold-doped germanium shows spectral structure associated with valence band intra-band transitions. For the lightly doped specimens, with increasing concentration, the structure in the spectrum becomes less pronounced. Newman and Tyler have reported studies of the same effect in gallium-doped germanium. Our studies indicate

that the effect is more pronounced in gold-doped germanium than in gallium-doped germanium.

When intra-band absorption is peeled off from the absorption spectra at 195° and 298°K, the threshold of absorption is at a higher energy for the higher temperatures.

The transmission of infra-red light through both pure and lightly gold-doped germanium is found to be enhanced by about 16 per cent at 4.2°K compared to that at higher temperatures ($> 60°K$). The determination of surface reflectivity at 4.2°K gives 0.29 and correspondingly a refractive index (μ) of 3.3 This shows an anomalous behaviour of $\frac{d\mu}{dT}$ at low temperatures. It is known that materials with the diamond structure reveal similar extra-ordinary behaviour in other lattice properties such as the temperature dependence of their coefficient of thermal expansion and Debye temperatures.

GRADUATE STUDIES

Field of Study: Physics

Physics of the Solid State	J.B. Gunn
X-rays and Crystallography	G. Bate
Elementary Quantum Mechanics	F.A. Kaempffer
Low Temperature Physics	J.B. Brown
Theory of Measurements	A.M. Crooker

Related Fields: Metallurgy

Topics in Physical Metallurgy	Department of Metallurgy Staff
Phase Transformation in Metals	W.M. Armstrong
Topics in Chemical Metallurgy	Department of Metallurgy Staff

Mathematics

Numerical Analysis	Charlotte Froese

PUBLICATION

Solid Solubility of Gold in Germanium, Canadian Journal of Physics, 40, 286 (1962).

Supervisor: Professor Robert Barrie

ABSTRACT

Tyler used Hall coefficient measurements to evaluate the gold acceptor concentration in germanium crystallized from a germanium-gold melt at a temperature between the melting point of pure germanium and 17°K below this temperature. The present study reports the results of similar measurements in the temperature range of growth from 12° to 80°K below the melting point of germanium. A crystal grower was designed and constructed for growing the monocrystals of gold-doped germanium.

It was found that the $\langle 100 \rangle$ direction was the most favorable direction for eliminating dendritic growth on gold-rich phase crystallized as inclusions. The phenomenon of retrograde solubility was observed. The maximum solubility ($\sim 2.8 \times 10^{16}$ gold acceptor atoms per c.c.) occurred at about 30°K below the melting point of pure germanium.

Infra-red absorption in gold-doped germanium was studied between 4.2° and 298°K over the energy range from 0.08 to 0.6 e.v. The magnitudes of the absorption cross-sections for the specimens containing about 3.5×10^{15} and 1.2×10^{15} gold acceptor atoms per c.c. were in close agreement with the data of Johnson and Levinstein. The cross-section of absorption near the band gap of germanium for the heavily gold-doped germanium ($> 10^{16}$ gold acceptor atoms per c.c.) is about the same as in the case of lightly doped specimens. Whereas in the case of lightly doped specimens, however, the cross-section of absorption drops sharply to negligible values as the energy of the incident photon decreases, the cross-section of absorption for the heavily doped specimen remains very high. The excess absorption is found to remain substantially the same when measurements are extended to the energy range between 0.032 and 0.044 e.v.

At 298°K, the absorption of infra-red radiation in gold-doped germaniun shows spectral structure associated with valence band intra-band transitions. For the lightly doped specimens, with increasing concentration, the structure in the spectrum becomes less pronounced. Newman and Tyler have reported studies of the same effect in gallium-doped germaniun. Our studies indicate that the effect is more pronounced in gold-doped germaniun than in gallium-doped germaniun.

When intra-band absorption is peeled off from the absorption spectra at 195° and 298°K, the threshold of absorption is at a higher energy for the higher temperatures.

The transmission of infra-red light through both pure and lightly gold-doped germanium is found to be enhanced by about 16 per cent at 4.2°K compared to that at higher temperatures ($\gtrsim 60^{\circ}K$). The determination of surface reflectivity at 4.2°K gives 0.29 and correspondingly a refractive index (μ) of 3.3. This shows an anomalous behaviour of $\frac{d\mu}{dT}$ at low temperatures. It is known that materials with the diamond structure reveal similar extra-ordinary behaviour in other lattice properties such as the temperature dependence of their coefficient of thermal expansion and Debye temperatures.

TABLE OF CONTENTS

LIST OF FIGURES

ACKNOWLEDGEMENTS

The author is grateful to Professor R. Barrie, Dr. J.W. Bichard and Dr. J.C. Giles for their kind encouragement and invaluable suggestions during the course of the work. He also extends appreciation to Mr. J.B. Gunn, Dr. G. Bate and Mr. P. Graystone for help during the preliminary stages of the work and to Mr. W. Morrison of the Machine Shop of the Department of Physics for the construction of some equipment.

The author is indebted to the External Aid Office of the Government of Canada for providing a scholarship under the Colombo Plan and to the Pakistan Council of Scientific and Industrial Research for granting study leave. The work was supported by the Defence Research Board of Canada grant number 9512-26.

PART 1

INTRODUCTION

Chapter I

Most semiconductors owe their conductivity to impurities, and these may be classified electrically as donors or acceptors. Two theoretical approaches have been used in discussing impurity states. One is the effective mass approximation; the other is a tight binding approximation.

Detailed application of the method of the effective mass to germanium has been made with particular reference to donor elements of Group V and acceptor elements of Group III in substitutional sites. The model used in these cases is that of an impurity center, such as As (valence configuration $4s^2 4p^3$) having one more electron (donor) or Ga ($4s^2 4p^1$) one less electron (acceptor) then is required to fill the bonding orbitals of the four tetrahedral germanium ($4s^1 4p^3$) neighbors. The extra electron, or the deficiency (hole), is considered to be bound to the impurity atom by an attractive Coulomb force, exerted on the electron or hole by the oppositely charged impurity atom, somewhat analogous to that of the hydrogen atom. This force is modified by the dielectric constant of the crystal. The influence of the lattice on the motion of the electron is taken into account by the use of an effective mass. These elements produce centers in germanium introducing localized energy levels into the otherwise forbidden energy gap that require about 0.01 ev for ionization of the carrier at $0^{\circ}K$.

The basic assumptions underlying the method just described are valid for the large orbits which are characteristic of small binding energies. The assumptions are not valid for the case of the impurities having deep levels discussed below. If, for example, we assume an ionization energy of 0.1 ev or more, an effective mass calculation indicates that a major fraction of the charge density of the excess electron will lie within one lattice spacing of the impurity atom. In other words, it lies within a region where the theoretical

procedure must be regarded as invalid. To the present time, however, there has not been any satisfactory theoretical treatment of energies and wave functions associated with deep levels.

Although a quantitative theory of the impurities having deep levels is not available, a similar consideration permits some rationalization of their behaviour. Consider, for example, the behaviour of the impurities Zn and Te. The valence configuration of Zn is ($4s^2$). If a Zn atom goes into solution substitutionally, it may be expected to form tetrahedrally oriented bonds with the neighboring germanium atoms. However, there are two electrons less than are required for tetrahedral bonding. Thus the Zn atom must accept two electrons to complete the tetrahedral bonding, that is, it may act as a double acceptor. The valence configuration of Te is ($5s^2 5p^4$). There are two electrons more than are required for tetrahedral bonding; in other words, the Te may act as a double donor. Elements such as Cu and Au having $4s^1$ and $6s^1$ configurations act as triple acceptors, as suggested by the tetrahedral bonding model.

The behaviour of gold in germanium may be described as follows (Figure 1) Dunlap (1955 a, 1955 b). At very low temperatures the 6s electron

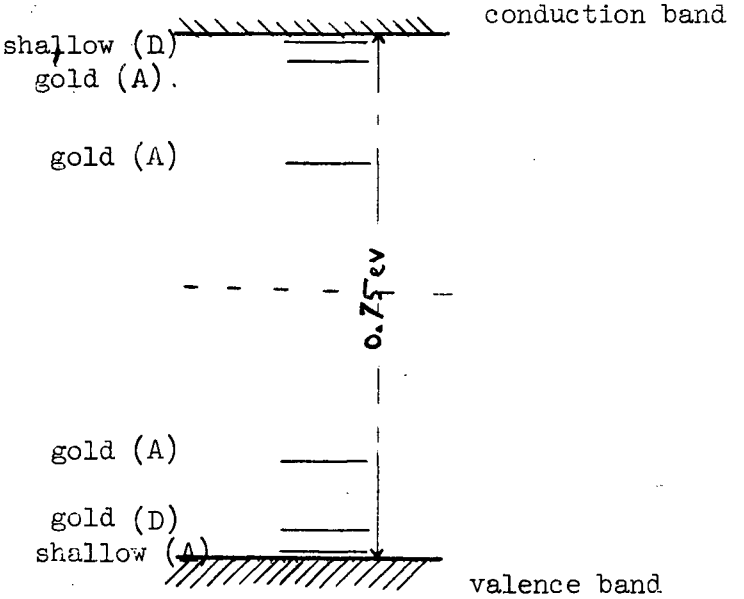

Figure 1. Gold and other (shallow) acceptors (A) and donor (D) centres within the band gap of germanium.

behaves as a donor 0.05 ev above the valence band, that is, the strength of bonding of this electron to an Au-Ge pair is less than the strength of bonding of an electron to a Ge-Ge pair by 0.05 ev. Because of the low-level of this donor state, it is not possible to see donor action directly due to gold in germanium, and the effects are seen only through trapping action upon p -type germanium doped with shallow acceptors. The three acceptor states represent the three unsaturated Au-Ge bonds. The first acceptor state is determined by the energy required to remove an electron from a nearby Ge-Ge bond and to place it on a neutral gold atom, or alternatively, the minimum energy ($\sim$0.16 ev) required to release a hole. The second is above the middle of the forbidden energy band (0.20 ev below conduction band). Because of the onset of intrinsic conduction, it is not possible for an appreciable number of electrons to be excited into these levels. Thus the only source of electrons for the upper level is to trap electrons from the higher acceptor or donor atoms containing available electrons. Thus the upper level is more properly termed an electron trapping level than an acceptor level. Because of the apparent equality between the number of upper and lower states, Dunlap (1955 A) suggested that the upper level is merely a second ionization state, in which an electron is added to the filled lower states. The gold ion would thus be Au^{--} when the upper state is filled, Au^{-} when the lower state is filled. Similarly, a high-lying 0.04 level below the bottom of the conduction band appears when both lower acceptor levels have been compensated. This is another ionization of the gold to form Au^{---}.

The need for semiconductor crystals containing accurately controlled amounts of impurities has stimulated interest in the variation with temperature of solid solubilities in these binary systems. The solubility of an impurity is the maximum concentration of the element possible in the germanium-impurity solid solution when the system is in equilibrium at constant temperature with

the molten host substance.

The general type of eutectic diagram is as shown in Figure 2.

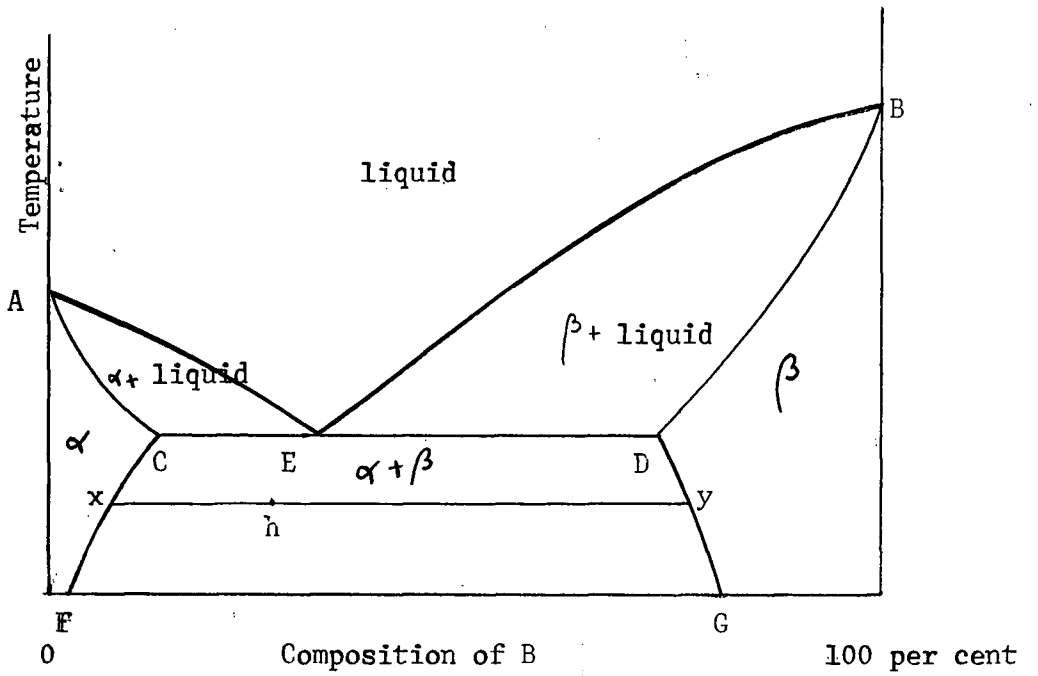

Figure 2. Equilibrium diagram for a eutectic system

In eutectic systems, the melting points of each metal are depressed by the addition of the other, and the two liquidus curves AE and BE intersect at the eutectic point E. The corresponding solidus curves are AC and BD and alloys below the curve ACDB are totally solid. Alloys in the region between the solidus and liquidus consist of a mixture of solid and liquid phases, and at any temperature the compositions of the two phases in equilibrium are given by the intersection of the temperature ordinate with the curve concerned. This is known as the lever principle. In the liquidus/solidus equilibrium, we may within limits choose the composition of the liquid phase, and once this choice is made the temperature and the composition of the solid are established. Alloys in the region ACE consist of liquid in equilibrium with the solid solution of B in A which may be called α , whilst those in the region BED consist of liquid in equilibrium with the solid solution of A in B denoted by β . At the eutectic temperature CED, liquid of composition E is

in equilibrium with α solid solution of composition C and β solid solution of composition D. Below the eutectic horizontal the alloys are totally solid, and alloys in the region FCEDG consist of a mixture of α and β solid solutions, the equilibrium composition at any one temperature being obtained by drawing a temperature horizontal; thus in Figure 2 an alloy h will, at the temperature shown, consist of a mixture of α of composition χ and β of composition y.

Thus the eutectic involves a continual increase in the composition of the solid solution as the solidus curve falls from A to C. This implies that as the temperature falls the lattice of the parent metal A can take up continually increasing amounts of B into solid solution so long as the equilibrium involved is with the liquid phase. It may, however, happen that as the temperature falls the lattice can no longer accommodate so many solute atoms, and in this case the solidus curve is of the form shown in Figure 3, and exhibits a maximum solubility somewhat below the melting point of A. This is the phenomena of retrograde solubility. Most impurities that have been studied have been shown to be retrograde in germanium (Burton, 1954).

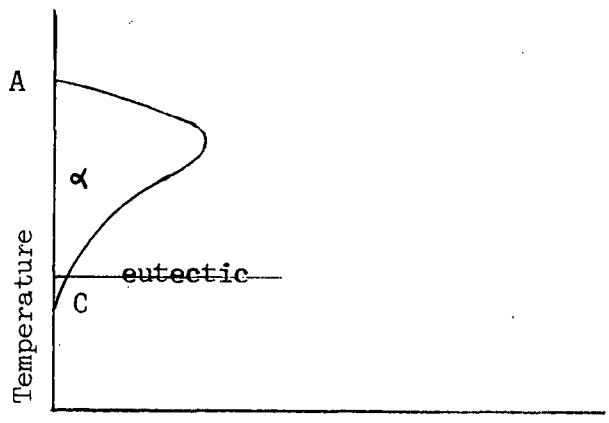

Figure 3.

A retrograde solidus curve.

Tyler (1959) used Hall coefficient measurements to evaluate the gold acceptor concentrations in germanium, crystallized from a germanium-gold melt at temperatures between the melting point of pure germanium and 17°K below this temperature. Baker and Compton (1960) measured the solid solubility of gold in vapor-grown germanium at about 530°K below the melting point using both radioactive tracer techniques and Hall coefficient measurements to evaluate the gold concentration. The results of Baker and Compton showed that the solubility obtained from radio-tracer measurements was forty times higher than that obtained from electrical measurements. Even the solubility obtained from electrical measurements was too high in comparison with other solutes in a crystal grown at that temperature. One of the purposes of this work is to study the solid solubility of gold in germanium crystallised from melt containing increasing concentrations of gold and consequently decreasing temperature of crystallisation determined by the germanium-gold liquidus diagram (Thurmond and Kowalchick 1960).

Important information about a semiconductor may be obtained by studying its infra-red properties. It is possible to correlate the infra-red properties with other properties of the material by studying different samples under various conditions. Infra-red absorption in a semiconductor is classified into four different types according to mechanism: intrinsic absorption, carrier absorption, absorption involving localized states, and lattice absorption.

By intrinsic absorption we refer to the absorption due to the excitation of valence electrons to the conduction band across the energy gap. It is reponsible for semiconductors being opaque and having metallic reflection in the optical region. At sufficiently long wave-lengths where the photon energy is insufficient to excite the electrons across the energy gap, the absorption becomes small and the radiation can be transmitted by bulk samples. The wave-

length at which this occurs is in the infra-red formost semiconductors.

The absorption produced by the free carriers may be observed in the infra-red beyond the edge of the intrinsic absorption. Optical transitions between two energy levels of the same band are forbidden by the selection rules. Therefore, free electrons can only be excited to energy bands above the conduction band and holes can only give rise to excitations of electrons from energy bands below the valence band. Unless the separations are small for the energy bands concerned, such excitations will not be possible in the infra-red region. The absorption by carriers depends then on disturbances in the periodic structure of the crystal (and hence relaxation of the selection rule), due to lattice vibrations or impurities and lattice defects. Since these factors are also responsible for the electrical properties of the material, there should be correlation between the latter and the carrier absorption. In germanium crystals there are a number of overlapping energy bands in the valence band. In such cases, infra-red absorption due to intra-band excitations of the free carriers is observed which gives useful information on the structure of energy bands.

The optical processes that may occur for acceptor and donor centers include (a) photoionization absorption involving transitions from the localized acceptor state to the valence band, and since localized states are associated with energy levels within the forbidden gap such transitions take place in the infra-red beyond the edge of the intrinsic absorption; (b) optical-excitation absorption involving transitions of the bound holes to a higher bound state, which should appear as narrow bands beyond the long-wavelength photoionization absorption limit. Energy levels and other information of interest for impurity and imperfection centers may be deduced from absorption studies.

The excitation absorption of Group III impurities in germanium has been seen before and recently (Fisher and Fan, 1960) experimental investigation has been extended to two acceptor impurities, Zn and Cu, of higher ionization energies. The absorption spectrum of neutral Zn^0, singly charged Zn^-, and neutral Cu^0 in germanium has shown structure attributable to excited states. Studies have been made on the singly charged Cu^- in germanium but no observation of the excitation lines have been reported. The line-width is determined mainly by the broadening of the ground state, and for germanium the ratio of the widths is expected to be (Lax and Burstein, 1955) of the order of the reciprocal of the Bohr radius squared. As the broadening of the ground state increases with decreasing orbit dimensions the failure to observe the excitation of Cu^- might be caused by large broadening.

The ionization absorption of Au in germanium has been observed before (Fan, 1956; and Johnson and Lewinstein, 1960) at 77°K but no observation of excitation lines has been reported. Since the line-width increases with temperature, excitation lines are most likely to be observable at low temperatures (e.g. 4.2°K). As mentioned earlier, excited states have been observed for singly ionised Zn^- (ionisation energy $\sim$ 0.09 ev) but not for singly ionised Cu^- (ionisation energy 0.33 ev). Neutral Au^0 happens to have an ionization energy (0.16 ev) lying between the above two and presumably also an intermediate Bohr "radius".

The effective mass formalism would not apply for the ground state but may still be valid for the excited states. The absorption spectrum measurements made at 4.2°K provides the means to check this assumption and to reveal effects due to differences in the ground states.

The organization of this thesis is as follows: In Part II we deal with the solid solubility of gold in germanium as a function of temperature. The intermediate range infra-red properties of gold-doped and pure germanium at different temperatures are discussed in Part III.

PART II. SOLID SOLUBILITY OF GOLD IN GERMANIUM

Chapter 2. Crystal Growing

To study the solid solubility of gold in germanium as a function of temperature, monocrystals have been grown by dipping a germanium seed in a melt containing germanium and gold in known proportions. Before the desired gold-doped germanium crystals could be prepared it was necessary to design and construct a crystal grower. The Czockralski withdrawal technique was employed in our method of growing gold-doped germanium crystals. This consists basically of a molten pool of the alloy, the temperature of which is controlled accurately at any value, and a seed of germanium monocrystal is held such that it can be rotated and lifted vertically at a slow rate.

The question of the purity of the additions is a crucial one in such a study as the present one. The gold used (99.999% minimum purity) came from Sigmund Cohn Inc. in the form of wire assayed by qualitative spectrographic analysis in the Lucius Pitkins Laboratories. It was checked for 25 elements suspected to occur naturally with gold. Of these only copper and silver were detected and these were present in concentrations less than 0.0009%. The germanium for these studies was initially in the form of a zone-refined bar having a resistivity of 50 ohm-cm. at 25°C. To reduce surface contaminants, the ingot material and the seed were etched in the mixture CP4 Medium having the following composition:-

Glacial Acetic acid	20 c.c.
Nitric acid (concentrated)	25 c.c.
Hydrofluoric acid (48%)	10 c.c.
Bromine	1 c.c.

The etchant was then rinsed off with de-ionized water. All water was then meticulously dried off the germanium using clean filter paper. The germanium was then stored in a desiccator before it was ready to be put into the crucible. Prior to use, the crucible was baked at 1200°C for fifteen minutes to drive off residual contaminants.

About 1/8 inch of the seed was dipped into the melt by lowering the rotating vertical shaft. After the seed was inserted into the melt, sufficient time and a high enough melt temperature was provided to assure complete melting of the original surface of the seed where it touched the liquid. A source of error arises if an appreciable portion of the seed crystal is dissolved in the melt. Care was taken to keep this at a minimum. The shaft with the seed crystal was then slowly raised, and at the same time the heat supplied to the melt was slightly reduced so that the temperature of the melt at that position might be just equal to the freezing point in order to prevent the seed crystal from melting away. In a normal freezing of an eutectic system a particle of the phase with the lowest surface energy will freeze out, this being that of the seed material. The diameter of the crystal during its initial growth was kept as small as possible to provide maximum opportunity for dislocations to grow out. This requires that the temperature of the melt be kept relatively high at first. The growth of the initial small diameter portion was maintained for a distance equal to several times its diameter (Dash, 1959). The melt temperature was then lowered to increase the diameter of the crystal.

The incorporation of impurity in the crystal may be characterized by a segregation coefficient. In treating a binary solution having solid and liquid phases, one may define an equilibrium segregation coefficient K_0 as the ratio of the concentration of solute in the solid C_s to that in the liquid C_L, when equilibrium exists between the two phases at a given temperature. When the solute composition of the system is decreased, so that the equilibrium temperature approaches the melting point of the pure solvent, K_0 converges to a constant value. With solutions of gold in germanium, $K_0 << 1$ ($K_0 = 1.3 \times 10^{-5}$, near the melting point of germanium (Tyler, 1959)). When crystallization occurs very slowly, the solid forming at any moment

from the melt has composition $C_s = K_o C_L$, provided one may assume diffusion in the solid to be negligible. As the crystallization proceeds, the rejection of solute by the solid enriches the melt. If the temperature of the crucible is held constant, then, as expected from the constitutional diagram (Figure 2) the interface rises from the surface, the melt holding on to the growing crystal by surface tension. The resulting interface is curved and the cross-section of the growing crystal progresively narrows. When a curved interface is obtained a radial temperature gradient will exist, thus causing cross-sectional variations of the impurity concentration. If the interface is flat, as is the case for a monocrystal growing with constant diameter, the impurity concentration is practically homogeneous over the entire cross-section (Dikhoff, 1960).

The crystal geometry was controlled by regulating the heat input to the system and the rate of withdrawal. When the desired crystal diameter was attained (about 1 cm.), the heat input to the system was regulated to keep the diameter uniform for the rest of the crystallization while it grew at a constant velocity equal to the pull velocity of the seed holder. Constancy of the diameter was considered to be indicative of a steady state.

It was assumed that diffusion in the solid was negligible, and mixing in the liquid was complete (that is, concentration in the liquid was uniform). These assumptions are discussed in the following.

Since gold has a very low diffusion coefficient in germanium ($\sim 5 \times 10^{-9} cm^2$ per second at 900°C, (Dunlap 1955a)), it is reasonable to assume that no change in concentration took place after crystallization due to transport in the solid state during the period of crystal growth (about three hours).

If crystallization does not proceed slowly, solute atoms are rejected by the advancing solid at a greater rate than they can diffuse into the bulk of the melt. The preparations of monocrystals containing high concentrations of gold was more difficult than the preparation of lightly doped materials. Assuming a segregation coefficient considerably less than unity the answer lies principally in the pile-up of the rejected impurity element in a depletion layer (depleted with respect to the semiconductor) adjacent to the solid-liquid growth interface. It is this solute-enriched region which directly determines the rate of solute incorporation into the solid. In order to pull a sound monocrystal it is necessary that semiconductor from the bulk melt enter this depletion layer, either by diffusion or mixing of some sort, at a rate equal to the growth rate of the crystal. Otherwise, dendritic growth or occlusion of liquid in the crystal results. In preparing heavily doped crystals it was necessary to grow from more heavily doped melts (that is, melts more dilute with respect to the semiconductor) so that it was more difficult to feed the semiconductor into the depletion layer at a sufficiently rapid rate. Hence, lower pull rates were required for the more heavily doped melts. At these low pull rates, small thermal or mechanical fluctuations which at the higher pull rates resulted in negligible growth rate fluctuations, now become of considerable importance. These heavily-doped crystals were grown with pull rates of 3×10^{-4} cm. per sec. and rotation rates of around 60 r.p.m. This ensured proper fluid flow conditions in the melt to give the effective segregation coefficient of gold its equilibrium value (Burton and Slichter, 1958).

A further complication is the effect of crystal orientation on the amount of impurity incorporated into the crystal. In the preparation of heavily doped materials the main concern was the preparation of sound monocrystals of the desired doping. Several different trial experiments were

made in which germanium seeds of $\langle 110 \rangle$, $\langle 111 \rangle$ and $\langle 100 \rangle$ were dipped and pulled from the melt containing germanium and gold. It was found that the $\langle 100 \rangle$ direction was the most favorable direction for eliminating dendritic growth or gold-rich phase crystallized as inclusions. This can be shown by noting that an ad-atom on a $\{100\}$ plane makes half its bonds with a completed underlying plane (2 bonds); whereas, a pair of ad-atoms on the $\{110\}$ plane are required to make half their bonds with each other and the underlying plane, and a trio of ad-atoms on the $\{111\}$ plane are required to make half their bonds with each other and the underlying plane (Bolling and Tiller, 1960). The small segregation coefficient and low solubility suggest that the gold atoms do not fit into the lattice too well. From the point of fundamental mechanism of the atomic kinetics of growth at the liquid-solid interface for diamond cubic lattice described above, it is likely that the incorporation of a gold atom in a diamond lattice is best facilitated in the $\{100\}$ plane in which case the ad-atom makes half its bonds with a completed underlying plane and are not required to bonds with each other; whereas in the cases of $\{110\}$ and $\{111\}$ growth planes multiple ad-atoms make half their bonds with the underlying plane and half with each other. In case the ad-atoms are gold, the chance to bond with each other results in the possibility of crystallization of the gold-rich phase.

When the gold concentration of the melt was too high, a gold rich phase occured in the crystal or there was extensive polycrystallinity. It was found that when the gold concentration in the melt was approaching an atomic fraction of 0.1, the mono-crystal character tended to deteriorate - first indications of lineage, in the form of numerous fine lines in the etched surface, appeared, and, in a fairly narrow belt, the crystal became poly-crystalline. This was studied after etching in a three percent solution of boiling hydrogen peroxide, which constitutes a useful slow preferential etchant.

This showed a large number of pockets containing metallic gold in this region of the crystal. By taking great care while regulating the heat input to the system in order to maintain a uniform diameter for the crystal and thus minimizing growth rate fluctuations, monocrystals free of lineage were grown from melts containing up to about 0.18 atom fraction of gold. The inclusions of the gold-rich phase increased towards the end last to freeze. Obviously, as the crystal was pulled, the gold content of the liquid was increased so that the number and size of the inclusions increased, and in the etched crystal fine parallel cracks began to appear when the germanium dissolved away.

The temperature of solidification was obtained from the relative concentrations of gold and germanium in the melt at different stages during growth. Instead of using the phase diagram, the liquidus curve evaluated from the liquidus equation was assumed (Thurmond and Kowalchik), and at known concentrations, the appropriate temperature at the interface was read off from the liquidus curve.

Four gold-doped germanium crystals were grown with different concentrations of gold in the melt. With a small amount of overlapping, these four crystals covered a range of temperatures from about 825°C to 925°C.

Chapter 3. Determination of concentration of gold acceptors.

3.1 Hall effect.

The Hall effect occurs when a substance carrying a current is subjected to a magnetic field perpendicular to the direction of the current. If the current is flowing in the x-direction and the magnetic field is applied in the z direction a field will appear across the sample in the y direction (Figure 4). This transverse field is found to be proportional to the product of the current density in the sample and the applied magnetic field; the constant of proportionality is called the Hall coefficient. This can be expressed as follows

$$E_y = R J_x H_z \qquad (1)$$

where E_y is the Hall field, J_x the current density, H_z the applied magnetic field and R the Hall coefficient. Usually the Hall coefficient is measured in terms of the transverse voltage produced by the transverse field between two directly opposite points on the sample. If the sample is a rectangular solid of thickness 'b' cm. and if the distribution of current is assumed uniform, (1) can be rewritten in terms of the total current J amperes, the Hall voltage V_H and the dimension of the sample

$$V_H = \frac{R J H_z}{b} \times 10^8 \qquad (2)$$

the magnetic field H_z being expressed in gauss.

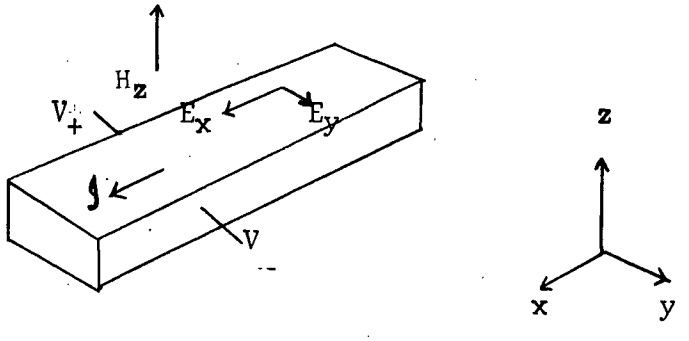

Figure 4. Voltage components for conduction by holes in a magnetic field.

3.2

Preparation of Specimens

Several thin slices were cut from the crystals perpendicular to their axes for maximum homogeneity. A wire saw was used for this purpose which cut the crystal by a reciprocating tungsten wire carrying a slurry of fine carborundum powder (#600) in grease. The cut slices were lapped on a ground glass plate using a water slurry of carborundum powder #600 to ensure flat and parallel faces. In general a high polish was not required.

The homogeneity was checked by exploring the resistivity over their surfaces with a four-point probe unit (Valdes, 1954). The resolution was somewhat limited by the point spacing (0.15 cm.). The variation measured was of the order of four percent.

After checks were made for crystal defects and homogeneity, as discussed in the foregoing, specimens were prepared for use in Hall coefficient measurements. The specimens used for Hall coefficient measurements had side-arm Hall contacts with dumb-bell ends and was cut out of the slice with a die (made of stainless steel) driven by an ultrasonic oscillator, cutting in a water-mixed slurry of boron carbide powder (#600) driven into the semiconductor by the motion of the tool. It is very important in this type of cutting to have the work firmly anchored to a backing plate free of air pockets, since otherwise the area of contact becomes small and any shifting results in cracking of the tiny filaments or bars. A suitable procedure was to mount the semiconductor blank on to a glass backing plate using Eastman 910 adhesive. The mounted slice was then left for about an hour at room temperature for curing. The semiconductor being cut was advanced against the cutting die by mounting it on a pivoted arm which was counter-balanced. By incorporating a dial gauge on the feeding mechanism and by knowing the thickness of the blank (about 0.03 cm.), it was possible to deduce from the dial reading when the tool had passed through the blank. The cut-out sample

was then detached from the glass backing plate by heating on a hot plate to about 100°C for about three minutes; this broke the Eastman 910 adhesive bond.

Current carrying contacts to the ends of the sample and electrical connections to the side-arms were made using the gold alloy technique. Bits of Eastman 910 adhesive were first removed by cautiously grinding the specimen with #600 carborandum on a ground glass plate. The samples were then cleaned by boiling in a 3 percent hydrogen peroxide solution. Great care was taken to avoid contamination of the samples. Immediately prior to alloying, the samples were etched in CP4.

The alloying was carried out by localized heating with a small michrome coil of the germanium cut-out in an inert atmosphere of flowing nitrogen. Gold (99.999 percent) wire of 0.005 in. diameter was cleaned of surface contaminants using alcohol (95 percent) and carried in glass dispensers. These dispensers were mounted in a pair of micromanipulators having a reduction ratio of four to one. The nichrome heater powered by a variable transformer was brought to the proper temperature which was judged by color. The wire was then brought into contact with the heated germanium which was gripped by a pair of self-locking stainless steel tweezers, the exact positioning of the contact being observed through a binocular microscope. Since gold and germanium form an alloy with an eutectic point around 350°C a small pool of alloy was formed which could be worked into the desired contact area. When this pool was slowly cooled (over about 30 seconds) some of the excess germanium recrystallized before the remaining alloy froze,using the underlying substrate as a seed.

After alloying the contacts, the specimens were dipped in boiling 3 percent hydrogen peroxide to remove any surface contamination.

The Hall potential probes were at a position no less then three sample widths from the end of a uniform sample so that negligible error was introduced due to short-circuiting of the Hall potential by the current contacts (Dunlap, 1950).

3.3

Measurements

The sample was mounted on a ceramic holder. It was supported only by the gold wire leads to minimize mechanical strain on the specimen and contacts. The holder was then fitted into a test tube for sample protection and positioning.

For measurements at moderately low temperatures the containing test tube was filled with glycerol and was immersed in a small dewar of freezing mixtures; the dewar fitted between the magnet pole pieces. The freezing mixtures used were common salt and ice, and ether and dry ice. The mounted sample was immersed in the dewar containing boiling oxygen and boiling nitrogen for measurements at these temperatures. The sample was allowed to warm up slowly from these temperatures by keeping only the dewar partly filled with the refrigerent while keeping the sample isolated in the test tube. With this apparatus, temperatures from that of room temperature down to 77°K could be achieved. The low temperatures were measured with a copper-constantan thermocouple placed in the proximity of the sample and connected to a potentiometer (Leeds and Northrup). With this it was possible to notice a change in temperature of 1°C. Over the period of time that was required to complete the measurement at a given temperature, no change in sample temperature was noted.

To provide temperatures above that of room temperature the mounted sample was put in a test tube filled with Varchlor and surrounded by a nichrome heater coil. The test tube with the heater was immersed in mineral oil inside the dewar. The heater temperatures were set and controlled electronically (Burgess, 1957) using a slice of n-type germanium as the temperature sensor. Temperatures from room temperature to about 100°C could be produced and maintained to within half a degree and over 100°C the control was within a degree. Two mercury-in-glass thermometors (graduated

from 15°C to 40°C in 0.05°C divisions and 0° to 200°C in 0.2°C divisions) were used to measure up to 200°C. For higher temperatures the copper-constantan thermo-couple was again used measuring temperature changes to within half a degree.

Ohmic contacts were necessary to avoid metal-semiconductor contact effects. An ohmic contact is defined as one which serves purely as a means for getting current into or out of the semi-conductor, but plays no part in the active processes occuring in the device. The following experiment was performed to test the current-carrying contacts. The overall resistance between the gold leads was measured as a function of current density in both directions at room and boiling nitrogen temperatures. The current was measured by a Weston Model 901 d.c. milliammeter in the range 0 to 1.5 mA. A potentiometer (Leeds and Northrup Model 8662) was used to measure the potential drop in the sample. No dependence on current direction was noted and also, no appreciable change of the resistance was observed when the current density was changed by a factor of 20 at each of the above temperatures. These were judged to be satisfactorily ohmic behaviour. The current density was well within the range of those used in Hall experiments.

To provide the magnetic field necessary for the Hall measurements, an electromagnet was used. It had flat pole pieces. They were 4 in. in diameter and had a gap of $2\frac{1}{4}$ in. between the pole pieces. The magnet coils were water-cooled. The electric current was supplied by a d.c. motor generator. To permit an accurate measurement of the magnet current a potentiometer (Leeds and Northrup), capable of measuring from 0.0 to 70.0 millivolts, was used to measure the potential drop across a Weston 0.25 milliohm resistor capable of carrying up to 200 amperes. The magnet was calibrated using a fluxmeter (Rawson type 504) and a search coil, and was checked by observing the nuclear magnetic resonance of lithium. The field was checked for homogeneity and was found to be satisfactory.

For most Hall coefficient measurements, the current was supplied by a power supply with a decade resistance box in series for regulation. The current was measured by a d.c. milli ammeter. A Rubicon model 2730 potentiometer capable of measuring from 0.000 to 0.161 volts or from 0.00 to 1.61 on a second scale was used for measuring Hall voltages. A switching system was included to permit rapid reversal of polarity in any current or potential lead.

In the measurement of the Hall voltage, certain associated effects give rise to potentials which must be corrected in order to avoid error in the measured value. The largest of these effects is the potential, V_{jR} , which appears because of the experimental difficulty in aligning the measuring probes on the same equipotential plane. Transverse or longitudinal thermal gradients can introduce unwanted potentials. A transverse gradient introduces a thermo-electric potential. In addition, there are three thermo- and galvano-magnetic effects. A longitudinal thermal gradient results in a longitudinal thermal flow which in the presence of the magnetic field produces a transverse Nernst potential or a transverse Righi-Leduc temperature difference which in turn gives a thermo-electric potential. The longitudinal current and the magnetic field produce a transverse temperature difference leading to an additional potential known as the Ettingshausen effect. If a series of four measurements is taken reversing the magnetic field and the sample current in all possible combinations then a method is available for elimating all the undesired associated effects except the Ettingshausen.

The Ettingshausen effect has associated a certain time delay which is required for the temperature gradient to become established. Due to the thermal capacity of the filament, this effect can be eliminated by a.c. measurements. Some test measurements were made using a Hall effect measurement circuit described by Dauphinee and Mooser (1955), and built in this laboratory (Jones, 1961). Such measurements were performed at a frequency of 35 cycles per second

on a few specimens covering the impurity range used and it was found that negligible error would result from using the d.c. measurements and ignoring this last effect.

3.4

Method of analysis.

The Hall effect provides a direct measurement of the carrier type and concentration. For the case of p-ytpe germanium, let us denote the density of heavy holes by p_1 and that of light holes by p_2. In the limit of strong magnetic fields the Hall coefficient attains a steady value (Williardson, Harman and Beer, 1954)

$$R_{H\to\infty} = \frac{1}{q(p_1+p_2)} \qquad (3)$$

where q is the magnitude of the electronic charge in coulombs. In this case, the extrinsic Hall coefficient is related only to the total extrinsic carrier concentration and involves no weighting factors containing mobilities. In applying this equation, exorbitant magnetic fields are not required for high mobility materials in order to obtain results which approximate the limiting values given by the equation (Harman, Williardson and Beer, 1954). The measurements were made at a magnetic field of about 20 kilogauss.

We now consider the problem of determining the concentration of acceptor centers, knowing the hole concentration as a function of temperature. Although in gold-doped germanium (p-type) the number of holes available is exactly the same as the number of states, such a situation is seldom realized. At low temperatures there are usually fewer available holes as there are donor atoms present as an unavoidable impurity. A number of donor atoms are ionized in filling up the acceptors. We let N_a , N_d denote the concentrations of acceptor and donor atoms respectively, N_a^-, N_d^+ the concentration of ionized acceptors and donors, and n_a, n_d the concentration of unionized acceptors and donors. It may be shown that the probability f of the lower gold acceptor level being occupied by electrons is given by

$$f = \frac{1}{\frac{1}{\beta}\exp\frac{\Delta E - E_f}{kT} + 1} \qquad (4)$$

where ΔE is the energy separation between the gold acceptor level and the top of the valence band, the energy E_f is called the Fermi level and acts as a normalizing parameter varying with temperature in such a way that the integral of occupied levels over the whole of the energy scale is equal to the number of electrons in the crystal and β is a statistical weight factor depending on the free energy due to electron spins in acceptor centers (Smith, 1959), k is Boltzmann's constant and T the absolute temperature.

The expression for f is not rigorously correct. It fails to take into account the ionization of the lower gold acceptor level when the gold donor is not completely filled. For the case in question, when any pair of the gold energy levels is separated by many times kT at all temperatures under consideration, it gives an accurate formulation of the problem.

We then have the concentration of ionized acceptors.

$$N_a^- = \frac{N_a}{\frac{1}{\beta}\exp\frac{\Delta E - E_f}{kT} + 1} \tag{5}$$

The number of unionized acceptors n_a is given by

$$n_a = N_a[1-f] = \frac{N_a}{1+\beta\exp\frac{E_f-\Delta E}{kT}} \tag{6}$$

We require the electrical neutrality of the system as a whole. The statement that the number of positive charges must equal the number of negative charges is expressed by the equation

$$p + N_d + n_a = n + n_d + N_a \tag{7}$$

$N_a > N_d$ and we consider only the region of partial ionization so that the Fermi level lies several times kT above the valence band and close to the impurity level. It is convenient to assume further that there is a sufficient number of acceptors present to give enough holes to suppress n, the electron

concentration, to a value much below the intrinsic value at sufficiently low temperatures. The suppression occurs because the law of mass action requires the product $n p$ to be constant, thus if p is increased by a certain factor, n is decreased by a reciprocal factor. Fortunately, in this condition, we may neglect the contribution from the free electrons as well as having n_d small and obtain for the equation which determines the Fermi level

$$p = N_a - N_d - n_a \tag{8}$$

We suppose that the equilibrium concentration of holes near the top of the valence band behave as free particles with effective mass m, taken to be 0.4 times the free electron mass (Lax and Mavroides, 1955), and are given by

$$p = 2\left(\frac{2\pi m kT}{h^2}\right)^{\frac{3}{2}} \exp\left(-\frac{E_F}{kT}\right) \tag{9}$$

Using (6) and (9), (8) reduces to

$$N_v \exp\left(-\frac{E_F}{kT}\right) = N_a - \frac{N_a}{1+\beta \exp\frac{E_F - \Delta E}{kT}} - N_d \tag{10}$$

introducing the notation

$$N_v = 2\left(\frac{2\pi m kT}{h^2}\right)^{\frac{3}{2}} \tag{11}$$

being referred to as the effective density of states in the valence band. By rearranging, (10) may be written as a quadratic equation for $\exp\left(\frac{-E_F}{kT}\right)$ namely

$$\frac{N_v \exp\frac{\Delta E}{kT}}{\beta N_v + N_d \exp\frac{\Delta E}{kT}} \exp\left(-\frac{2E_F}{kT}\right) + \exp\left(-\frac{E_F}{kT}\right) - \frac{\beta(N_a - N_d)}{\beta N_v + N_d \exp\frac{\Delta E}{kT}} = 0 \tag{12}$$

and so the Fermi energy is determined by

$$\exp\left(-\frac{E_f}{kT}\right) = \frac{-1+\left[1+4\left\{N_v \exp\frac{\Delta E}{kT}\right\}\left\{\beta(N_a-N_d)\right\}\Big/\left(\beta N_v + N_d \exp\frac{\Delta E}{kT}\right)^2\right]^{\frac{1}{2}}}{2N_v \exp\frac{\Delta E}{kT}\Big/\left(\beta N_v + N_d \exp\frac{\Delta E}{kT}\right)} \qquad (13)$$

We evaluate E_f in two limiting situations. First we suppose

$$\frac{4\left\{N_v \exp\frac{\Delta E}{kT}\right\}\left\{\beta(N_a-N_d)\right\}}{\left(\beta N_v + N_d \exp\frac{\Delta E}{kT}\right)^2} >> 1$$

corresponding to large N_a or low T.

We have then approximately

$$p = \left\{\beta N_v (N_a - N_d)\right\}^{\frac{1}{2}} \exp\frac{-\Delta E}{2kT} \qquad (14)$$

We note that, under the above approximate conditions, straight lines are obtained of slope equal to half the (negative of the) ionization energy ΔE, when $k \ln p$ is plotted against $\frac{1}{T}$.

In a second limit we suppose

$$\frac{4\left\{N_v \exp\frac{\Delta E}{kT}\right\}\left\{\beta(N_a-N_d)\right\}}{\left(\beta N_v + N_d \exp\frac{\Delta E}{kT}\right)^2} << 1$$

corresponding to small N_a or high T.

Now we have approximately

$$p = \beta N_v \frac{N_a - N_d}{N_d} \exp\left(-\frac{\Delta E}{kT}\right) \qquad (15)$$

Care must be taken, however, in doing this since a binomial expansion of the square-root of the right-hand side is permissible only under the above conditions. In this case the slope of a plot of $k \ln p$ against $\frac{1}{T}$ involves only the (negative of the) ionization energy ΔE. It is thus seen that the slope of the line obtained from plotting $\ln p$ against $\frac{1}{T}$ is either $\frac{\Delta E}{k}$ or $\frac{\Delta E}{2k}$, depending on the degree of compensation.

We have obtained an experimental curve of $\ln p$ as a function of temperature by measuring the Hall coefficient R over a range of temperatures. Because in the germanium under consideration only gold is deliberately introduced, gold is the dominant impurity and the product is always p-type. The extraneous donor density present as a compensating impurity will be of negligible amount. This may be tested from the slope of the $\ln p$ against $\frac{1}{T}$ curve mentioned above. Under this approximate condition, that is when N_d is very small so that $\frac{N_d}{p} \exp \frac{\Delta E - E_f}{kT} \ll p \ll N_a$ we have approximately

$$N_a - N_d = p + p^2 (2\beta)^{-1} \left(\frac{2\pi m kT}{h^2}\right)^{\frac{3}{2}} \exp \frac{\Delta E}{kT} \qquad (16)$$

obtained from (12). The (negative of the) slope of a plot of p versus $p^{\frac{3}{2}} \left(\frac{2\pi m kT}{h^2}\right)^{-\frac{3}{2}} \exp \frac{\Delta E}{kT}$ gives $\frac{1}{\beta}$. This value of β can then be used to obtain the gold acceptor concentration in germanium from (16), utilizing, say, room temperature Hall coefficient data.

3.5

Results

a) Influence of shallow acceptors and donors.

The method given in the previous section for finding the gold acceptor concentration assumed that other impurities have negligible influence on the electrical properties. The possibility of misinterpretation, based on fortuitous addition of impurities due to contamination arising in the furnace during growth was precluded by the following considerations.

Denoting by the subscript 'f' any foreign impurity

$$\left(\frac{C_f}{C_{Au}}\right)_{crystal} = \frac{K_f}{K_{Au}}\left(\frac{C_f}{C_{Au}}\right)_{melt}$$

where C's denote concentrations and K's segregation coefficient. For deep-lying impurities $\frac{K_f}{K_{Au}} \lesssim 1$, so that their presence in the crystal can be discounted. However, shallow impurities have a high segregation coefficient compared with that of gold and relatively small traces of these in the melt could lead to relatively larger concentrations in the grown crystals.

The carrier behaviour of gold-doped germanium may be described as follows. The 6s electron behaves as a donor 0.05 ev above the valence band. Gold can give up this electron to low-lying empty levels and thereby become Au^+. When the sample is heated from 0°K to higher temperatures, the gold levels initially possess the charge Au^+. About the temperature 100°K, most of the electrons that had been trapped by the shallow acceptor states are re-excited to the gold levels and these become Au^0. We see that at higher temperatures the gold donor levels add no free carriers, and their primary effect is that of a trapping state. Because of the low level of the gold donor state, it is not possible to see donor action directly due to gold in germanium, and the effects are seen only through the trapping action upon p-type germanium.

On going to temperatures higher than about 100°K the electrons in the valence band have enough energy to be excited directly to the lowest gold acceptor level and the gold becomes Au^-.

Because in the germanium under consideration only gold is deliberately introduced, the product is always p-type. The extraneous donor density present as a compensating impurity will be of negligible amount. This may be tested from the slope of log p against $\frac{1}{T}$ curve, (Figure 5) in the manner mentioned in the previous section, in the deionization region of lower

to follow page 26

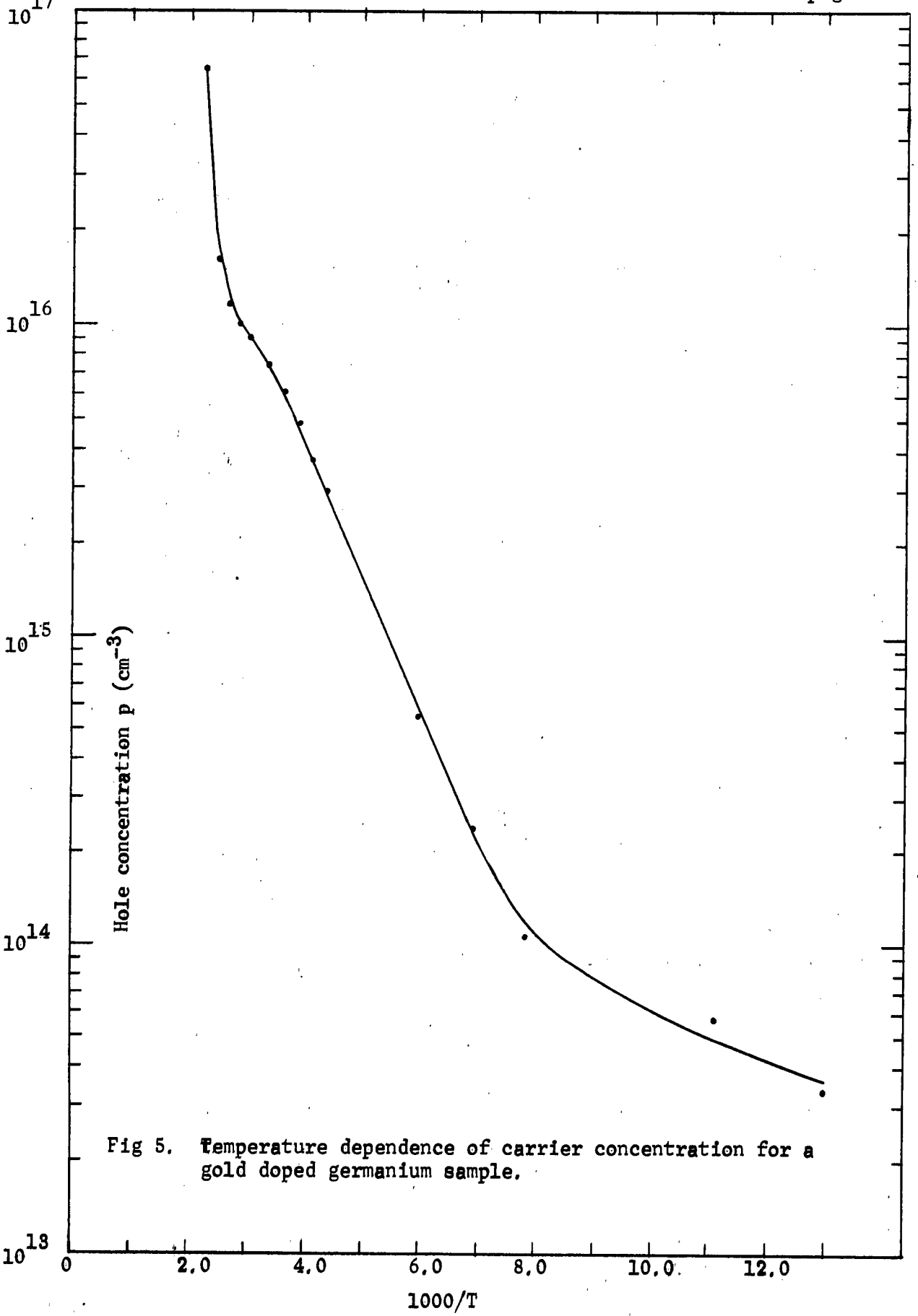

Fig 5. Temperature dependence of carrier concentration for a gold doped germanium sample.

acceptor centers of gold. The slope of the straight line in this region is doubled to give 0.14 ev as the ionization energy fulfulling the approximate conditions of (14), and thus $N_d \ll p \ll N_a$. The estimation of the ionization energy is further discussed in the next sub-section.

It is interesting to note that, due to the amphoteric action of gold in germanium, information about accidental shallow acceptors can also be obtained from the shape of the curve $\log p$ against $\frac{1}{T}$ entering the ionization region (under 125°K) of the 0.05 gold donor level. We have seen that at lower temperatures the 6 electrons from the gold donor level compensates the impurity centers that are located at the lowest energy levels through trapping action. When the sample is heated from 0°K to higher temperatures, the gold levels initially possess the charge Au^+. About the temperature 125°K, most of the electrons that had been trapped by the shallow acceptor states are re-excited to the gold levels and these become Au°, the shallow acceptor states being simultaneously filled by electrons from the valence band. Alternatively, as the temperature is raised, electrons are excited from the valence band with increasing ease into the vacated Au^+ levels; if $N_{Au} > (N_a - N_d)_{shallow}$, excitation of electrons occurs into the $(N_a - N_d)_{shallow}$ vacated gold levels. In either case, the gold donor states are entirely filled by about 125°K with an ionization energy ~ 0.05 ev and there remain $(N_a - N_d)_{shallow}$ holes in the valence band at this temperature; the crystal is p-type. From Figure 5, the Hall coefficient near 125°K gives $(N_a - N_d)_{shallow}$ approximately 10^{14}. If $(N_a - N_d)_{shallow} > 0$ the gold donor level is filled as described above, and an electron will not be excited into gold acceptor level of the particular gold atom until the gold donor level for that atom is filled. That is, the gold donor level is almost completely filled with electrons near 125°K and the gold acceptor level has not yet started to fill, so that there are $(N_a - N_d)_{shallow}$ holes (the 0°K

population of A_u^+), in the valence band at these temperatures. If shallow $N_d >$ shallow N_a, the gold donor level would not be active at any temperature and there would be no holes in the valence band due to this gold donor level. From the above discussion we see that the foreign shallow acceptor concentration is greater than the foreign shallow donor concentration, and that both of them are negligible compared to the gold concentration.

At temperatures below 125°K, the ionization energy of the gold donor level can be obtained from the slope of the log p versus $\frac{1}{T}$ curve of Figure 5. A value of 0.048 ev is found using the approximate conditions of (14). This is in good agreement with the values between 0.041 and 0.05 found by other workers (Dunlap 1955B, Klein and Debye 1960, Holland and Paul 1962). A major simplification implied in the use of the above mentioned analysis is that, because the ionization energy of the gold donor is large in comparison both to kT and to the ionization energy of the shallow acceptors, we can neglect the statistical effect of the shallow acceptor states and regard them as part of the valence band.

Similar curves for samples with different gold concentrations were of the same general form.

b) Determination of ΔE.

In Figure 6 a plot is shown of $k \ln (pT^{-\frac{3}{4}})$ against $\frac{1}{T}$ for one sample rather than $k \ln p$ against $\frac{1}{T}$. It is approximately a straight line in the deionization temperature range from 300° to 125°K. The slope has been used to obtain the value for ΔE for gold acceptors in germanium. We note that, under the approximate conditions of (14), the slope of the straight line is doubled to give $\Delta E \sim 0.14$ ev in good agreement with the value of 0.16 ev reported by Tyler which is used in the calculations. Low temperature infra-red studies of the absorption edge corresponding to ionization, which is presented later, confirmed the value used for ΔE.

to follow page 28

Fig 6. Plot of k $\log_e(pT^{-3/4})$ against 1000/T for a gold doped germanium sample (the same as used for figure 5).

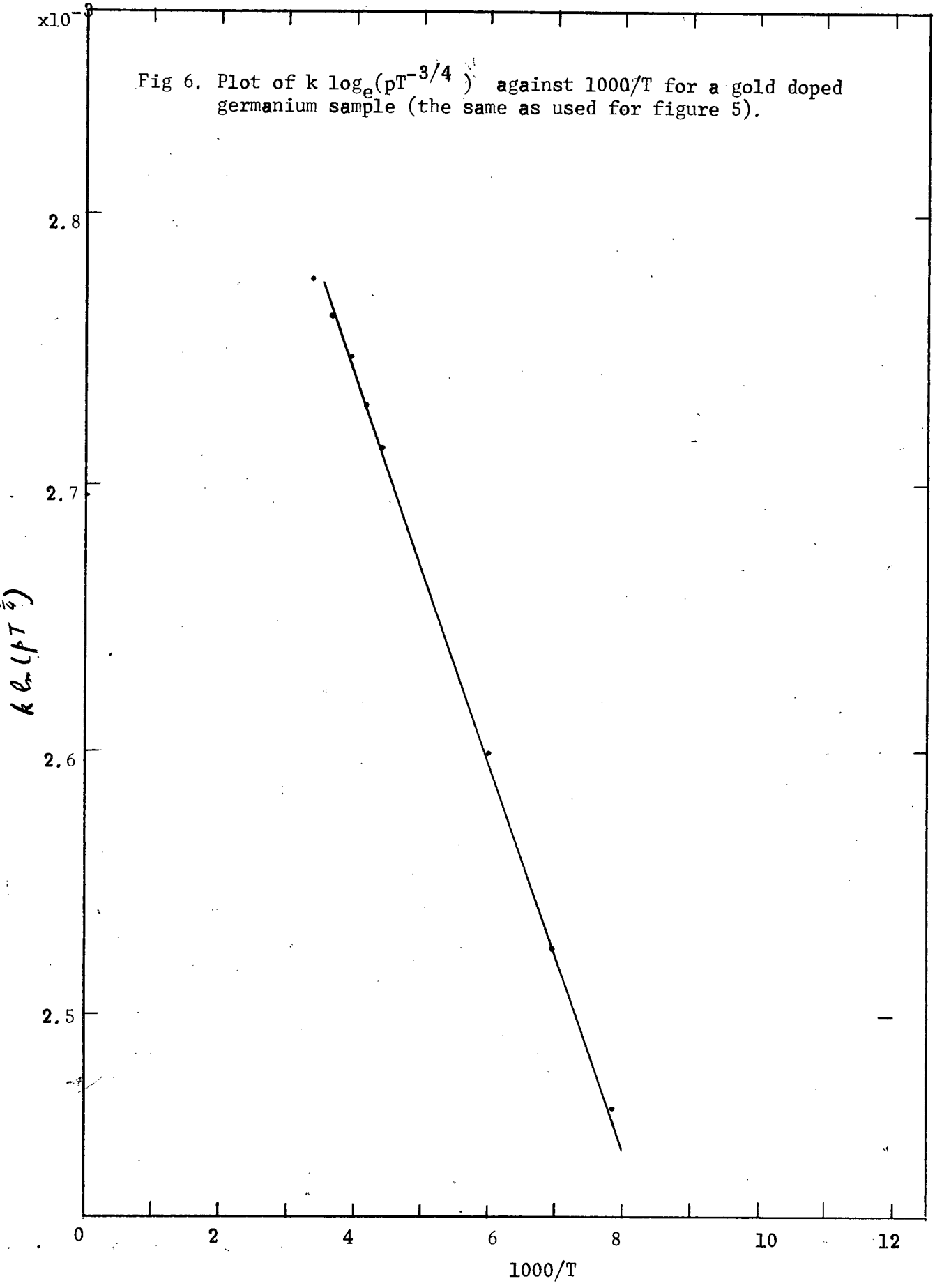

c) Determination of β.

A plot of p versus $\frac{p^2}{2}\left(\frac{2\pi m k T}{h^2}\right)^{-\frac{3}{2}} \exp \frac{\Delta E}{kT}$ is shown in Figure 7. The slope gives an approximate value of β as $\frac{1}{2}$. This is in agreement with that reported by Brooks(1955), rather than 8.5 reported by Klein, Debye and Ruprecht (1960).

d) Determination of N_a.

Figure 8 (Syed, 1962) shows values of N_a plotted as a function of temperature (degrees below the melting point of germanium) derived from the Hall coefficient studies using (16). The main source of error is due to fluctuation in the magnetic field which is about 4 per cent. The contribution of this and other errors (such as in the specimen thickness and the temperature) to the final value is about $\pm$ 10 per cent.

The results of Tyler have been included in Figure 8 for comparison. The phenomenon of retrograde solid solubility is observed as expected. The maximum solubility of gold ($\sim 2.8 \times 10^{16}$ atoms per c.c.) occurs at about 30°K below the melting point of pure germanium. The solubility decreases exponentially at lower temperatures.

to follow page 29

Fig.7. Plot of p vs $\frac{b^2}{2}\left(\frac{2\pi m k T}{h^2}\right)^{-\frac{3}{2}} \exp\frac{\Delta E}{kT}$ for a gold doped germanium sample (the same used for figure 5)

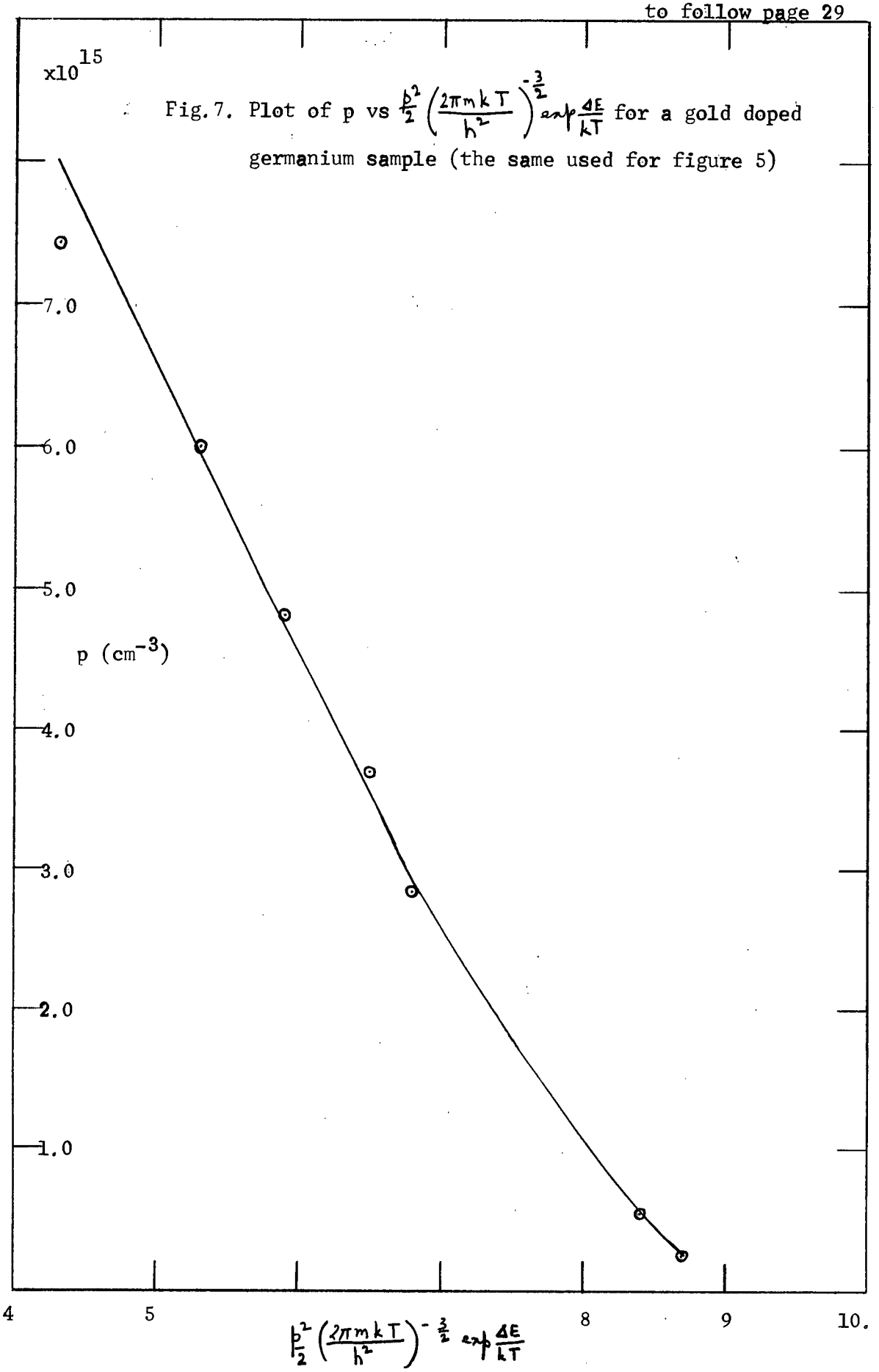

to follow page29

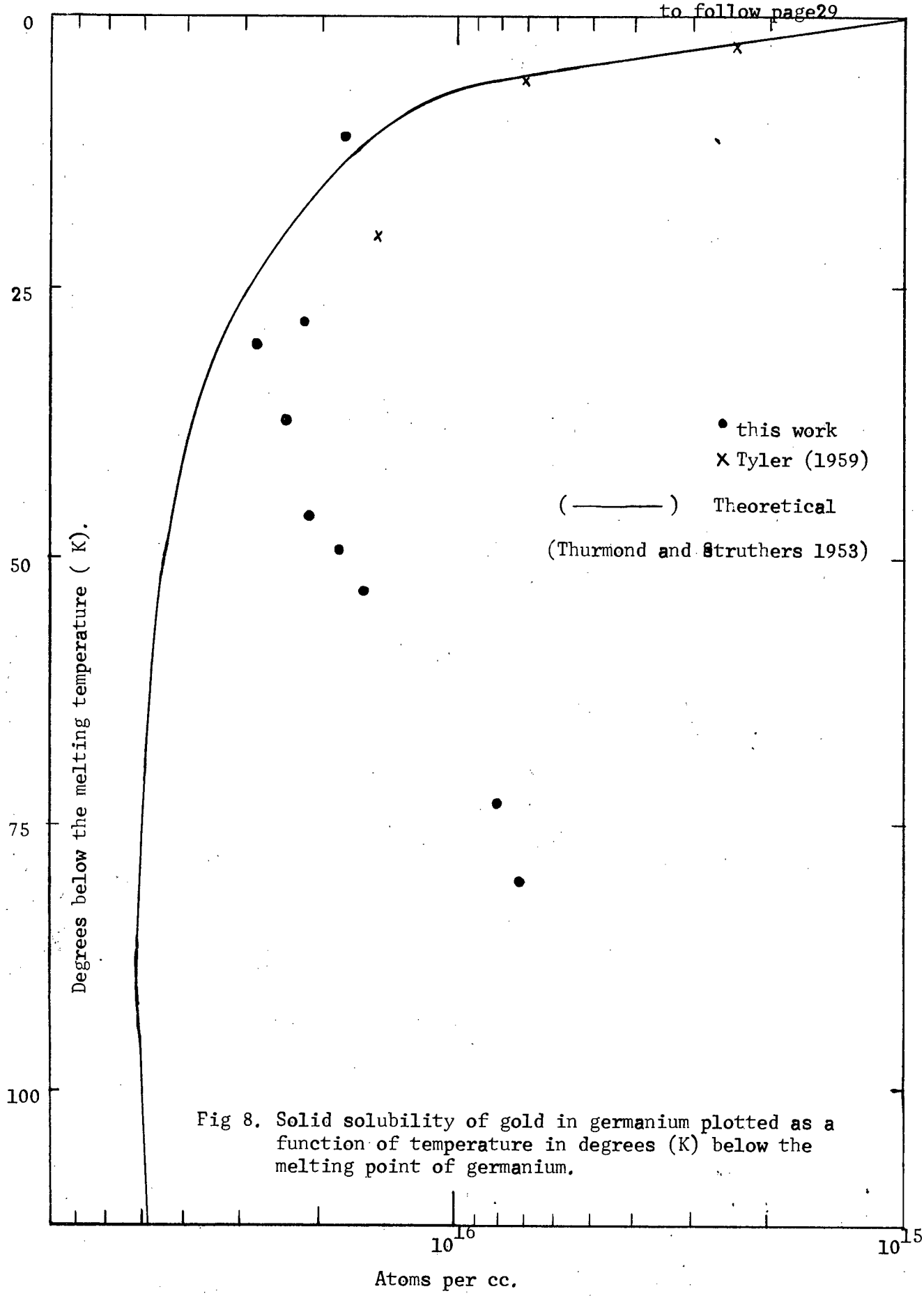

Fig 8. Solid solubility of gold in germanium plotted as a function of temperature in degrees (K) below the melting point of germanium.

Chapter 4. Theoretical calculation of segregation coefficient.

The thermodynamical relations determining the variation of segregation coefficient and solubility with temperature have been discussed by Thurmond and Struthers (1953) and by Kozlovskaya and Rubinshtein (1962). The equation derived by Thurmond and Struthers was obtained in the following manner.

The reference state of the impurity was taken as the solid impurity at its melting point. The change in chemical potential in terms of enthalpy and entropy differences was then expressed for the transfer of impurity atoms to the host crystal to a concentration C_s on the one hand, and into the molten host material to a concentration C_ℓ on the other hand. By setting the chemical potentials of the impurity in the host crystal and in the melt equal to each other it was possible to solve the equation for the ratio $\frac{C_s}{C_\ell}$, which, by definition, is equal to the segregation coefficient K. In this manner the authors arrived at the following expression:

$$\ln K = \frac{T_{1f}}{T} \ln K^* + \frac{\Delta S_f}{R}\left(\frac{T_{1f}}{T} - 1\right) \qquad (17)$$

where T_{1f} is the melting point of germanium (1210°K), and K* the segregation coefficient at the melting point of germanium. ΔS_f is the entropy of fusion at the melting point of the solute. The entropies of fusion of most metals do not differ much and 3 cal. per deg. was taken as representative (Kelly, 1935).

The solidus curve was calculated from (17) and plotted in the same figure[8] with the experimental values. Good correspondence is observed between the calculated and experimental values for crystals grown from dilute solutions. The temperatures corresponding to maximum solubility do not agree and the rate of decrease of solid solubility is much higher than calculated for crystals grown with increasing concentrations of gold in the melt. For crystals grown at about 80°K below the melting point of pure germanium, the discrepancy between the calculated values of the solubility and the experimental data from electrical measurements is up to an order of magnitude. It is possible

that this discrepancy is due to a crystallographic arrangement different from that of the primary solid solution, such that each of one element forms more bonds with the other element and fewer with its own kind. Such an arrangement constitutes an intermetallic compound and is further discussed in Part III. The intermetallic compound tends to form at the expense of the primary solid solution. Since we are dealing here with a molecular bond no electrical effect due to it can be expected.

Recently Kozlovskaya and Rubinshtein obtained a thermodynamic relation almost similar to (17) by taking the vapor pressure of the dopant as a measure of the chemical potential.

PART III. INFRA-RED STUDIES

Chapter 5. Experimental

5.1 Apparatus and Procedure.

A modified Model 12B Perkin Elmer Spectrophotometer which has a single beam double-pass monochrommator equipped with 60° rock salt prism was mainly used for the infra-red studies. Figure 9 shows the optical path of the instrument. Radiation from the Globar source S_o was focussed on the variable width entrance slit S_1 of the mono-chrommator by the plane mirror M_1 and spherical mirror M_2 . The portion of the beam which passed (path 1) through the entrance slit was collimated by the off-axis paraboloid M_3 and a parallel beam was refracted by the prism P. The Littrow mirror M_4 returned the radiation which was refracted again by the prism. Energy was focussed by the paraboloid in the dispersed field in the vicinity of the entrance slit (path 2). A portion of the field was intercepted by mirror M_5 and came to a focus between the halves of split mirror M_6. M_6 reflected the beam (path 3) back through the system, slightly displaced so that, after a second traversal through the parabola-prism-Littrow system, it was brought (path 4) to a focus on the exit slit S_2, after reflection from M_7. Near the entrance slit the energy was modulated by a semi-circular chopper (CH) at a frequency of 13 cycles per second. The exit slit passed chopped radiation of a narrow energy range of photons whose band width depended on the slit width and whose mid-band energy depended on the Littrow angle setting. The energy interval of photons which passed through S_2 was focussed with the help of the spherical mirror M_8 and plane mirror M_9 onto the specimen; the transmitted energy was then collected and focussed on the detector by the ellipsoid M_{10} producing a pulsating signal which was proportional to the intensity of the beam. An evacuated high-speed thermocouple provided with a caesium iodide window was employed as the detector. The pulsating electro-motive force at the thermocouple was amplified by a

to follow page 32.

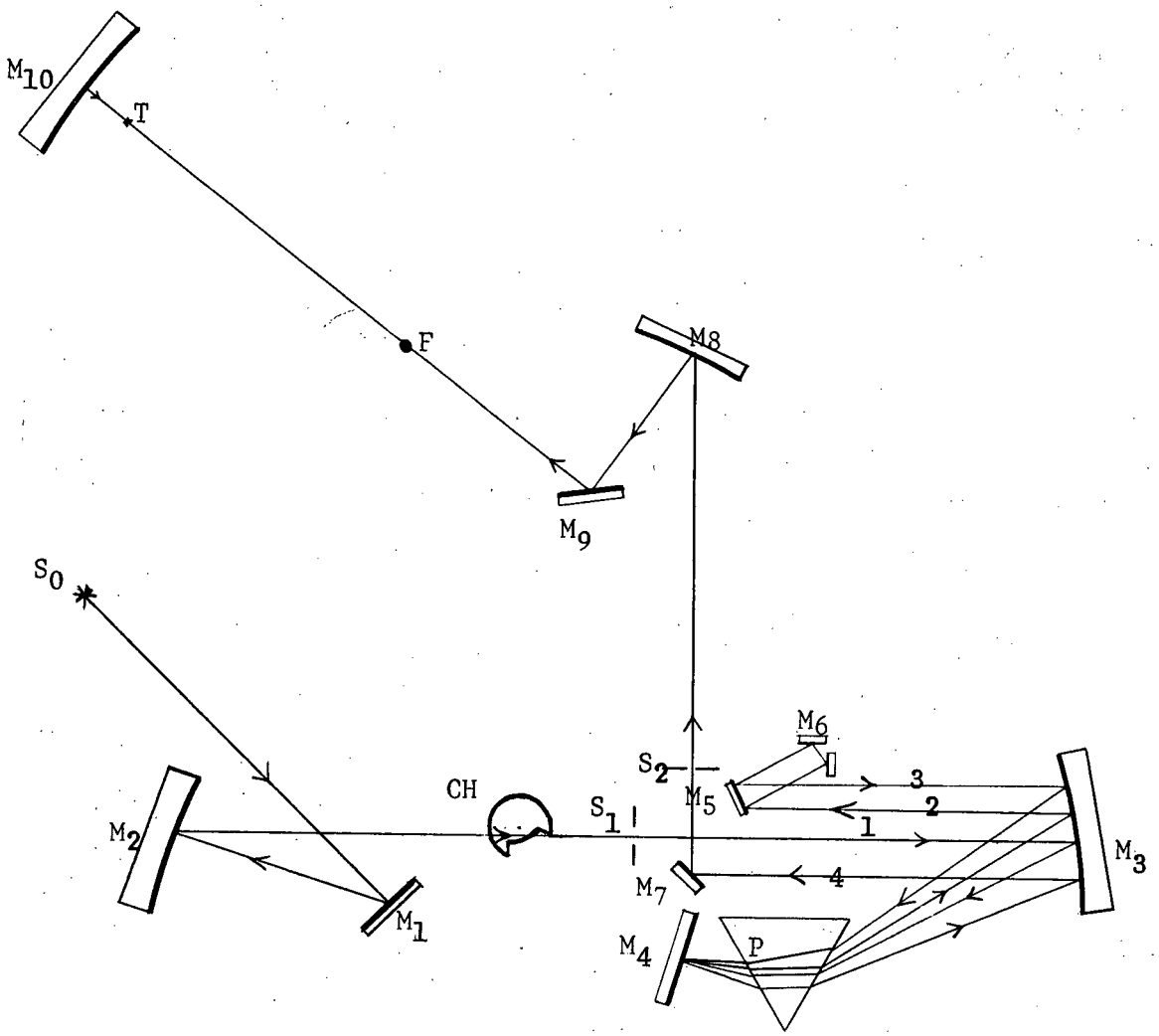

Fig.9 Optical path of modified Perkin Elmer model 12B single beam infra-red spectrometer with double pass monochromater

13 cps amplifier (Parkin Elmer Model 107). The chopped radiation signal was rectified by breaker-type synchronous rectifiers, actuated by rotations of the chopper shaft. The amplified signal was recorded by a Honeywell electronic potentiometer on strip chart.

The characteristics of the Perkin-Elmer thermocouple were:-

The minimum radiation flux observable with the detector under given conditions (sensitivity): 4 microvolts per microwatt.

Response time: 75% of d.c. response at 13 cps modulation,

Target size: 0.2 x 2 mm.,

Resistance: 12 ohms.

In each burst of light the number of photons was very small compared to the total number of gold atoms in the specimen. During the time interval when the radiation was stopped by the chopper blade, the sample returned to equilibrium. Thus no saturation effects occured.

The effective transmission limit of the monochromator was 0.08 ev, imposed by absorption in the prism material. When working at photon energies less than about 0.16 ev, the intensity of scattered radiation of higher photon energies was reduced by using a Kodak series 230 Far Infra-red Filter, through which the transmission of radiation of energy greater than 0.4 ev is under 3%. The remaining high energy photons merely contributed to the continuous background, and was within experimental error the same through a pure and doped specimen. Any possible heating of the specimen due to the radiation is negligible as well.

The spectrometer was calibrated by identifying the absorption bands of atmospheric water vapor, carbon dioxide, ammonia, (Oetgen, Kao Chao-Lan and Randall, 1942), and caesium iodide (Plyler and Phelps, 1952). In the course of a measurement dry nitrogen gas, obtained by boiling liquid nitrogen, was blown continuously to reduce the absorption due to atmosphere water vapor and carbon dioxide.

The experiments consisted of measuring the transmission ratios of gold-doped germanium and pure germanium as functions of the energy of the incident photon for various temperatures and concentrations of gold-doped germanium.

The measurements were made at the temperatures corresponding to the boiling points at atmospheric pressure of helium (4.2°K), nitrogen (77.4°K), oxygen (90.1°K), at the temperature of dry ice (195°K), of pumped nitrogen (60±3°K) and at room temperature (298° ± 2°K). The refrigerants were contained in a metal cryostat vessel, the base of which was located near a focus of the radiation leaving the monochommator. The radiation ports were covered with rocksalt windows. Parallel-sided specimens were attached to a flat copper block at the base of the coolant container, with facilities for rotating alternatively the doped or a pure specimen into the path of the radiation. Thermal contact between the copper block and the specimens was achieved by means of vacuum grease containing a suspension of silver dust of grit number 325.

The specimens were held in place by a flat copper strip with a hole in its center for the passage of the radiation. Care was taken to avoid straining the specimens.

The specimens were cut transverse to the direction of crystal growth (to maximize homogeneity) with the help of a wire-saw from monocrystal ingots grown by the Czochralski technique. The specimen surfaces were ground on glass with slurries of progressively finer grades of boron carbide powder and polished on a polishing wheel covered by Selvyt polishing cloth of medium nap with boron carbide powder of grit number 600. The final polish was on Selvyt with levigated alumina (Linde B abrasive). Before mounting in the cryostat, the surfaces were degreased in an ultrasonic cleaning bath containing acetone.

Gold acceptor concentrations in the lightly doped specimens were determined from the resistivity of each specimen measured by the four-probe method appropriately corrected for thickness (Valdes). Their resistivities at room temperature were 1.4 ohm-cm. and 3.5 ohm cm. giving hole concentrations of 2.50×10^{15} per c.c. and 1.05×10^{15} per c.c. respectively (Hemmat and MacDonald, 1961). Using (16) these figures yield estimated gold acceptor concentrations of $3.5(\pm 0.15) \times 10^{15}$ per cc and $1.2(\pm 0.1) \times 10^{15}$ per cc respectively. They had thicknesses of 0.24 cm. and 0.36 cm. respectively. The variation in the acceptor concentrations indicated above is derived from the variation in resistivity of $\pm$ 0.2 ohm-cm. from one end of the specimens to the other.

The evaluations of the concentration of gold acceptors in samples adjacent to the heavily doped specimens used were carried out using Hall coefficient measurements (Part II) yielding 2.6×10^{16} and 1.7×10^{16} per c.c. of gold acceptor atoms. The first specimen had a thickness of 0.45 cm. (and was nearly the largest thickness to be readily accommodated in the available cryostat). It was later cut into two of thicknesses 0.14 cm. and 0.26 cm. The one of latter concentration was 0.22 cm. thick.

The following clarification may be in order. At first the infra-red studies were carried out on specimens containing over 10^{16} gold acceptor atoms per c.c., revealing certain extraneous absorption (described subsequently). In order to understand the nature of this excess absorption it became necessary to perform absorption studies on lightly-doped (containing about 10^{15} gold acceptors per c.c.) specimens which were not anticipated. The lightly-doped monocrystals were thus grown later and instead of determining the gold acceptor concentrations in the adjacent samples by Hall-effect, four-probe resistivity measurements were performed directly on the specimens used for the infra-red studies.

The monocrystals were found to have a dislocation density of about 2×10^4 to 4×10^4 per cm.^{2}.

The specimens used in the present investigation were thick enough that interference fringes could not be observed with the resolution available.

The absorption of radiation can be described in terms of an absorption coefficient α_ν such that the amplitude of the light wave of frequency ν decreases in the ratio 1: exp $(-\alpha_\nu d)$ in traversing a layer of thickness d. The monochrommatic absorption coefficient α_ν was obtained from the expression for the energy transmitted by a plate with parallel faces at normal incidence, taking into account multiple reflections, given by

$$t = \frac{(1-r)^2 \exp(-\alpha_\nu d)}{1-r^2 \exp(-2\alpha_\nu d)} \qquad (18)$$

where r is the reflectivity of the surface. The transmission of the pure material beyond the intrinsic absorption edge is then given by

$$t_o = \frac{1-r}{1+r} \qquad (19)$$

Hence the transmission ratio of doped to pure germanium becomes

$$\frac{t}{t_o} = \frac{(1-r^2)\exp(-\alpha_\nu d)}{1-r^2 \exp(-2\alpha_\nu d)} \qquad (20)$$

This is the ratio that was obtained by arithmetical reduction from the basic data measured in a typical experiment. Some experiments were also performed determining the transmission for a doped specimen relative to air using (18) which reduces to

$$t = (1-r)^2 \exp(-\alpha_\nu d), \quad \alpha_\nu d > 0.2 \qquad (21)$$

However, there are several advantages to the first method. The exact value for the reflectivity is considerably less important for calculating the absorption coefficient in (20) rather than when (18) is used. In addition, scattered high energy photons can be expected to be more nearly the same and

thus cancel in the ratio, when the doped specimen is compared to an intrinsic one, rather than with no specimen in the light path. Determination of surface reflectivity r was made for pure and gold-doped germanium by observing the maximum transmission in the transparent region of the spectra. Under these conditions $\exp(-\alpha_i d) \sim 1$ and r was calculated using (19), giving 0.36 ± 0.02 for temperatures above $60^{\circ}K$. Within experimental error the reflectivity remained constant over the region of incident photon energies under study (0.08 ev to 0.6 ev) and the temperatures investigated except at $4.2^{\circ}K$.

In the preceding outline for the calculation of the absorption coefficient, it was assumed that a parallel beam of light is at normal incidence on a parallel-sided specimen. Actually, the light beam was not parallel. However, since the maximum angle of incidence in the converging beam was only 8°, no correction for convergence was needed to be applied (Born and Wolf, 1959).

The values obtained for the spectral slit width with the slit widths employed were 3×10^{-4}, 1×10^{-3} and 5×10^{-3} ev at 0.14, 0.21 and 0.35 electron volts respectively. The intensity limited resolving powers $\frac{\lambda}{d\lambda}$ with the slit widths employed were about 30, 100, 300 and 200 at 3, 4, 7 and 12 microns respectively.

Transmission measurements on some heavily doped specimens were also taken between photon energies of 0.032 ev and 0.044 ev with a Perkin-Elmer spectrometer modified to house a Bausch and Lomb grating with 30 grooves per millimeter blazed at 30 microns in the first order. The intensity of higher energy photons was reduced by sooting the mirror in the entrance optics and by using two reflections from calcium fluoride plates. This reduced the higher energy photons to less than 3% of the total (Colbow, Bichard and Giles, 1962).

5.2

Results and Discussion of Errors

Transmission measurements were made on several specimens differing in thickness and gold concentration. It was most convenient to plot the measured transmission ratio, $\frac{t}{t_o}$, draw a smooth curve through the experimental points and select smoothed values of $\frac{t}{t_o}$ from which to calculate $\alpha_\nu (cm^{-1})$. Using the above procedure graphs of absorption coefficient $\alpha_\nu (cm^{-1})$ against energy (ev) of incident photons were obtained.

Results from measurements on specimens, containing 3.5×10^{15} per c.c. and 1.2×10^{15} per c.c. of gold acceptor atoms, at 77°K, 195°K and 298°K are shown in Figures 10, 11 and 12 respectively.

Figures 13 and 14 show the absorption in heavily doped specimens containing over 10^{16} per c.c. of gold atoms at 4.2°K, 77 °K, 195°K and 298°K.

In all cases lattice absorption (Briggs, 1952 and Simeral 1953) has been subtracted.

One source of error is the presence of some background vibrational lines due to atmospheric water vapor. Incomplete cancellation of the rather strong water vapor vibrational absorption band may be responsible for some uncertainty in the infra-red transmission.

The smoothed curve from which α_ν's were calculated was an average obtained by taking a very large number of measurements. Thus the bands in the graphs of $\alpha_\nu (cm^{-1})$ against photon energy (ev) involve judgment as well. For the lightly doped specimens, the accompanying fluctuations in a particular value of $\frac{t}{t_o}$ give corresponding fluctuations for the calculated α_ν's of 0.03 $cm.^{-1}$ about the plotted average. This seems to depend upon the accuracy with which each reading of basic data (t and t_o) can be made in the midst of amplifier noise. For the rather large absorption in the heavily doped materials (in which case (21) is used), the fluctuation is 0.3 $cm.^{-1}$.

to follow page 38

Fig 10. Absorption coefficient of gold doped (lightly doped) germanium vs photon energy at 77 K.

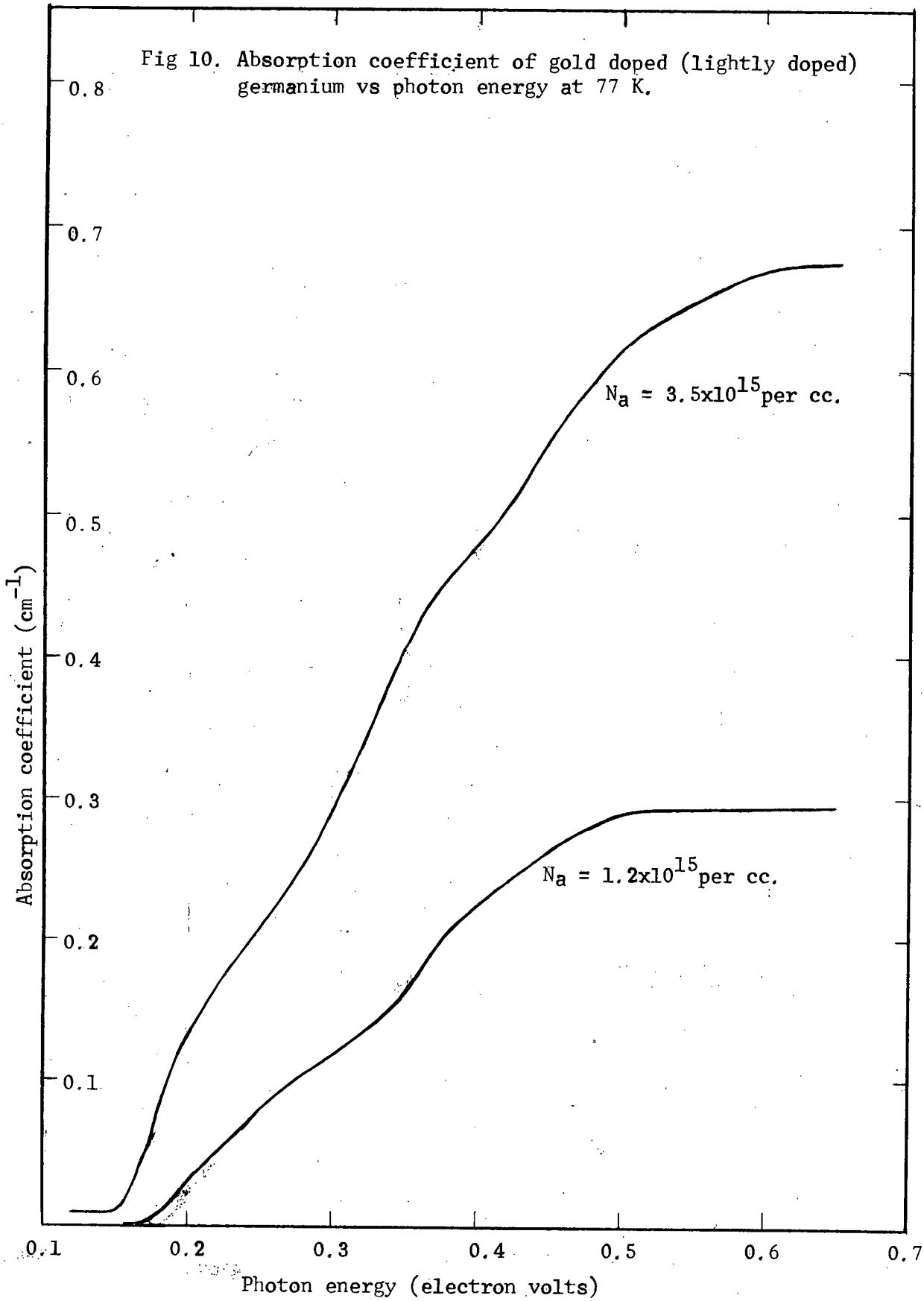

to follow page38

Fig 11. Absorption coefficient vs photon energy for gold doped (lightly doped) germanium at 195 K.

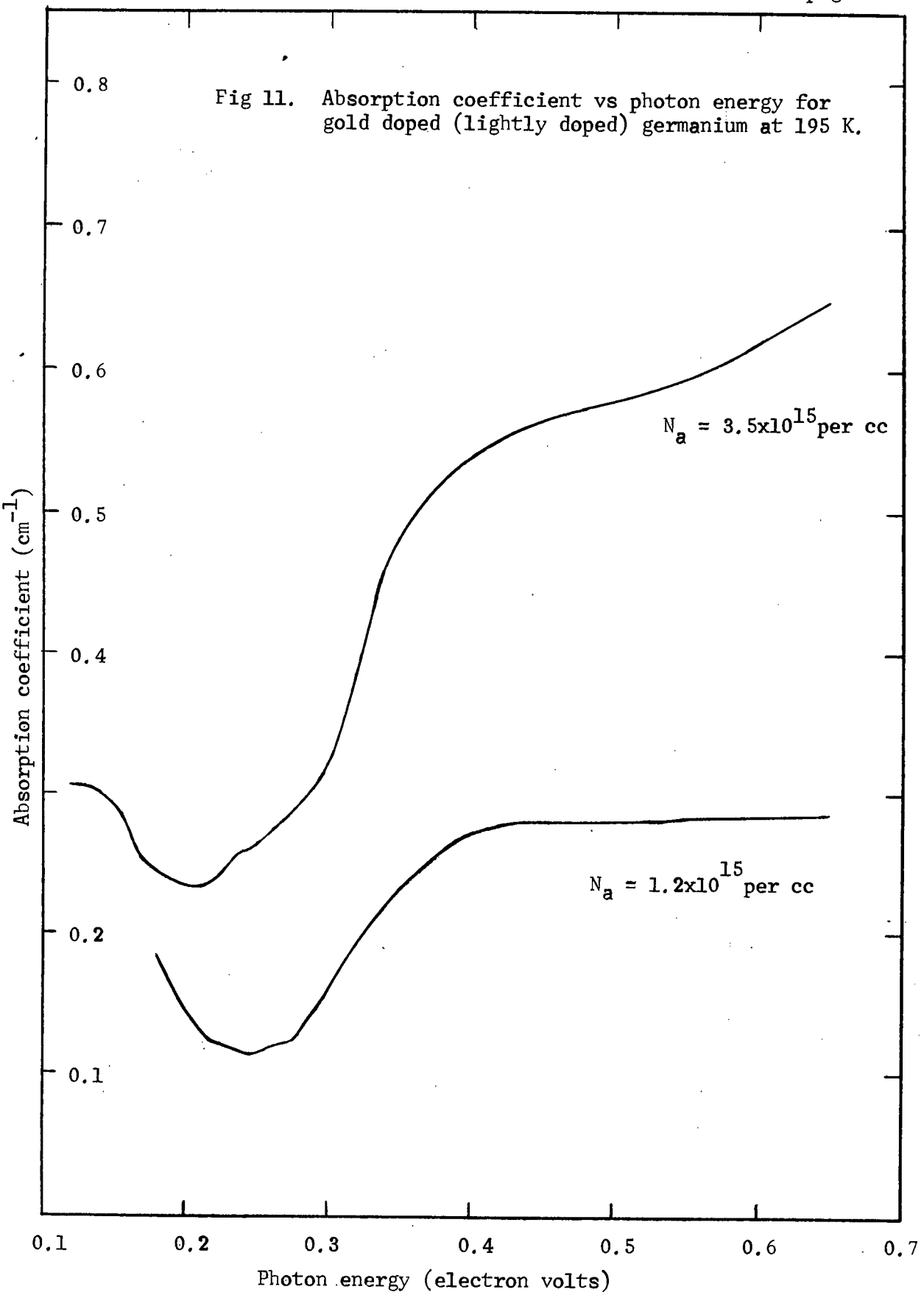

to follow page 38

Fig 12. Absorption coefficient vs photon energy for gold doped (lightly doped) germanium at 298 K.

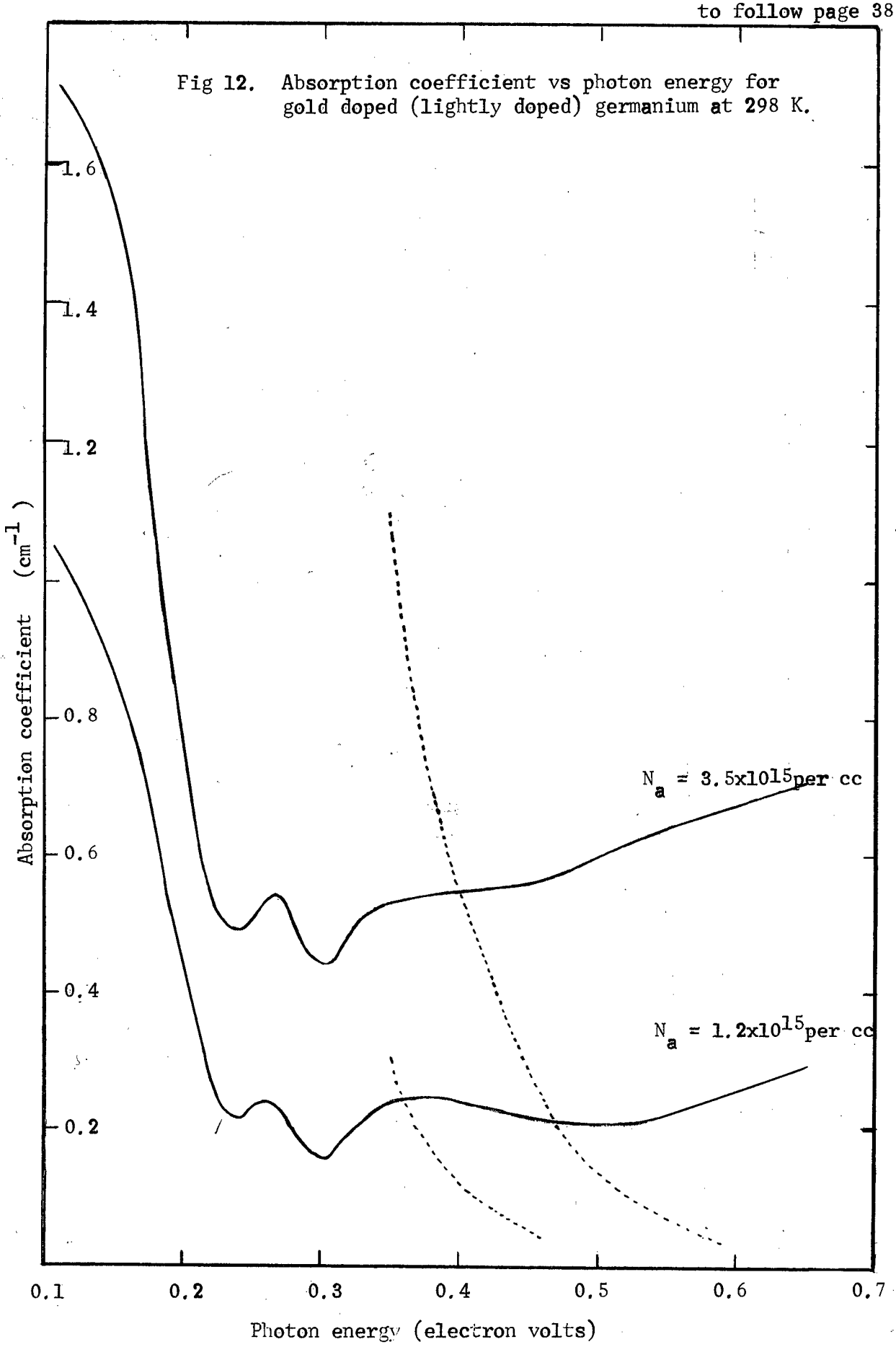

to follow page 38

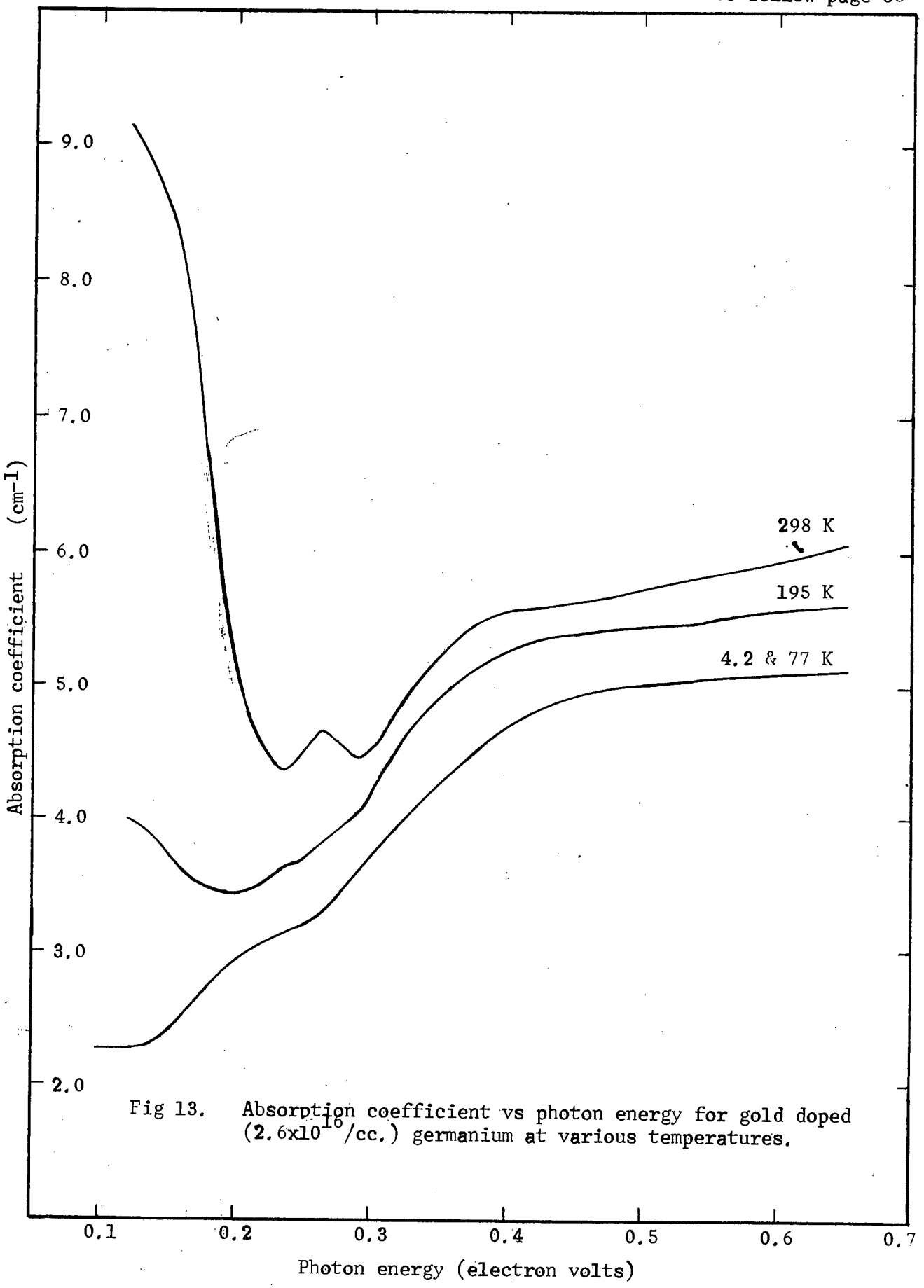

Fig 13. Absorption coefficient vs photon energy for gold doped (2.6×10^{16}/cc.) germanium at various temperatures.

to follow page 38

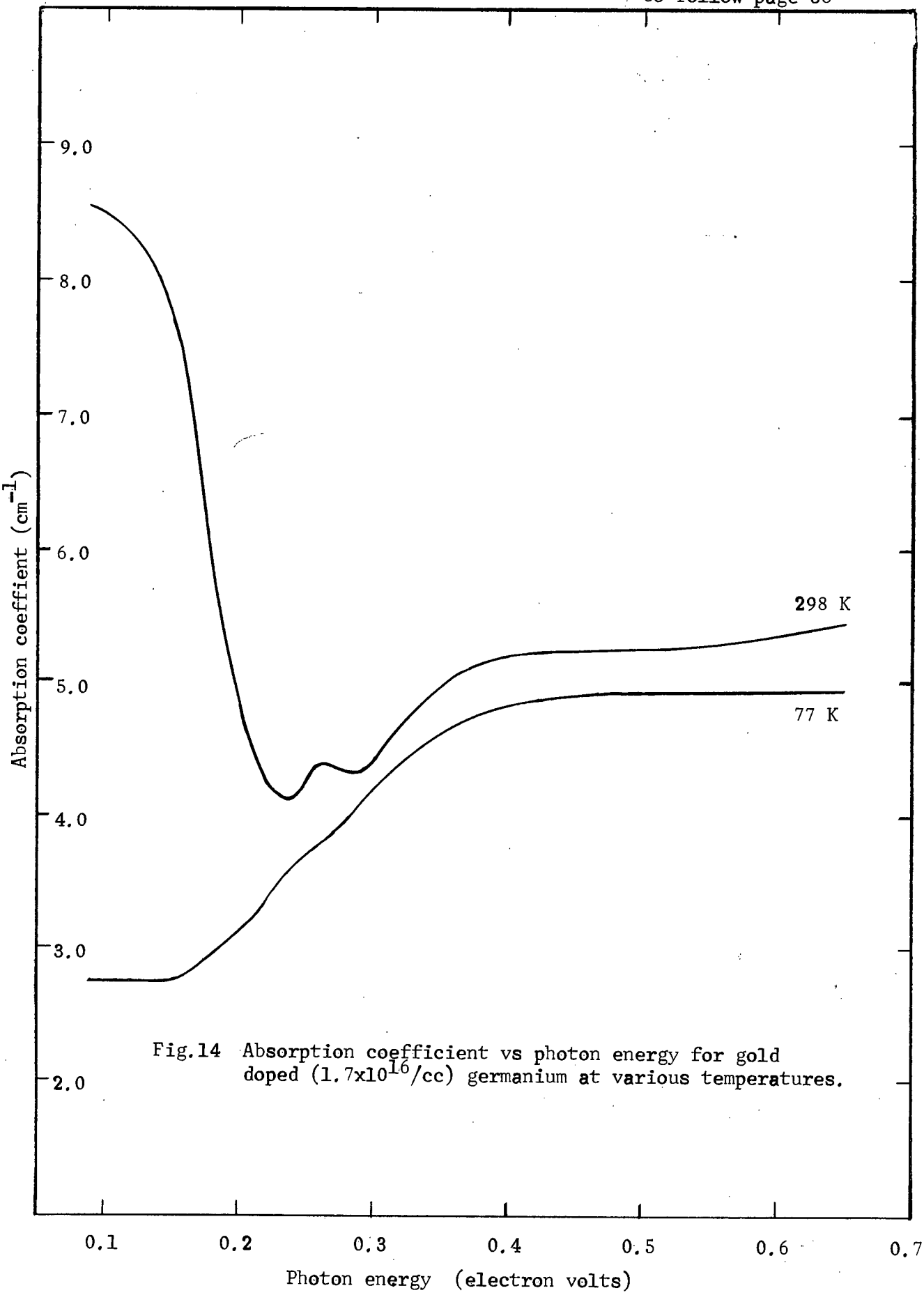

Fig.14 Absorption coefficient vs photon energy for gold doped (1.7×10^{16}/cc) germanium at various temperatures.

Chapter 6. Interpretation of Data

6.1 General

The absorption spectra at 77°K of the specimens containing about 3.5×10^{15} and 1.2×10^{15} gold acceptor atoms per c.c. is shown in Figure 10. In Figure 15 the absorption coefficient α has been divided by the gold concentration to obtain a cross-section and a comparison of results of this investigation (marked by *) and those of previous investigations (Johnson and Levinstein 1960; Fan, 1956)is shown. The magnitude of the absorption cross-section is in closer agreement with the data of Johnson and Levinstein. Each absorption curve shows a distinct rise near 0.16 ev, the energy corresponding to the first ionization of the gold acceptor center and continues to rise throughout the observed region. Johnson and Levinstein proposed that the absorption continuum to higher energies at sufficiently low temperatures arises from the vertical hole transitions from 0.16 ev acceptors to valence band states which are far removed from the center of the Brillonin zone at k=0. A hole bound to a deep acceptor implies a greater spread in k-space than a hole bound to a shallow group III acceptor. Localizing a hole on a 0.16 ev gold acceptor to a radius appropriate to an absorption cross-section of 2×10^{-16} cm^2. requires momentum components Δk in the bound hole wave function as follows: $\Delta k = \frac{1}{\Delta r}$ (from Heisenberg's uncertainty principle)

$$\sim \frac{1}{(2\times 10^{-16})^{\frac{1}{2}}}$$

$$\sim 10^{8} \text{ cm.}^{-1}$$

in k-space, that is, all the way to the zone boundary. The absorption to higher energies at sufficiently low temperatures would represent then the shape of a valence band energy surface (probably the heavy mass band) between points well removed from k=0 and the zone boundary. The transitions are shown schematically in Figure 16(a). In contrast, in shallow acceptors bound holes

to follow page 39.

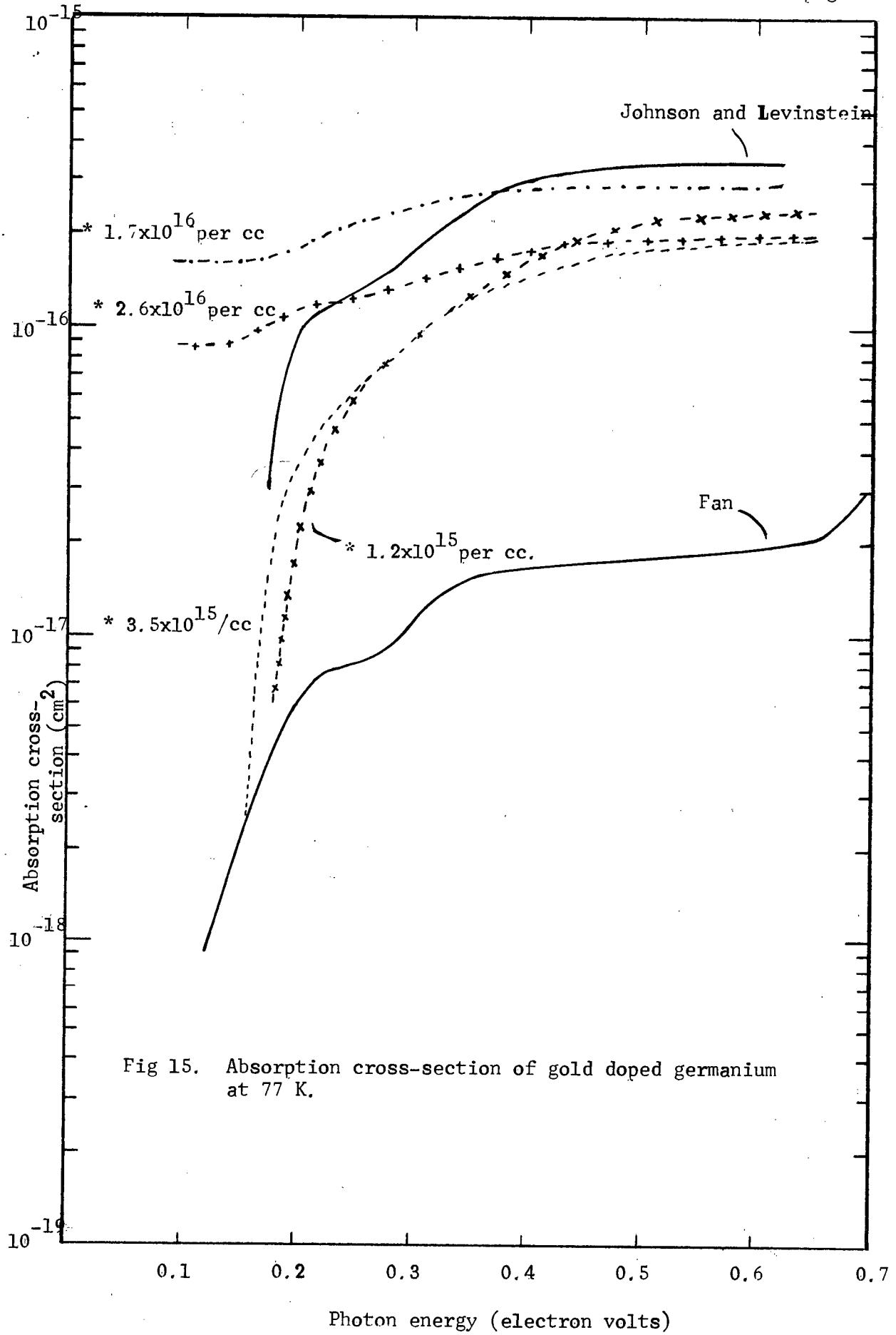

Fig 15. Absorption cross-section of gold doped germanium at 77 K.

possess, according to Johnson and Levinstein, wave vector components extending only to 10^7 cm^{-1}. Fan (1956) on the other hand suggested that the rise in absorption to higher energies is caused by the excitation of electrons from the V_3 band to the acceptor level.

Figure 12 shows absorption as a function of photon energy at 298°K. In Figure 17 the absorption coefficient α has been divided by the free hole concentration obtained from room temperature resistivity measurements to obtain a cross-section and a comparison of results of this investigation (marked by *) with those of previous investigations (Johnson, Levinstein ; Fan, 1956) is shown. Here again the magnitude of the absorption cross-section is in closer agreement with the data of Johnson and Levinstein. A comparison of the absorption spectra at room temperature of gold-doped germanium and p -type germanium doped with group III acceptors (Briggs and Fletcher, 1953) is also shown in Figure 17.

At 298°K, the absorption of infra-red radiation in gold-doped germanium shows spectral structure. Figure 12 shows the absorption curve of the specimen containing about 3.5×10^{15} gold acceptor atoms per c.c. At 298°K, 2.5×10^{15} holes per c.c. of these are free and give rise to absorption associated with valence band intra-band transitions. Only one weak band is observable at 0.26 ev followed by a smoothly rising absorption beginning around 0.23 ev. On the high energy side gold-doped germanium exhibits a rise in absorption beginning at 0.3 ev and an additional rise in absorption at 0.47 ev which extends on to the main absorption edge at 0.65 ev. The specimen containing about 1.2×10^{15} gold acceptor atoms per c.c. (1.05×10^{15} holes per c.c. in the valence band at 298°K) exhibits a dip in absorption beginning at 0.36 ev and then continues to rise at 0.5 ev extending on to the main absorption edge at 0.65 ev.

to follow page 40

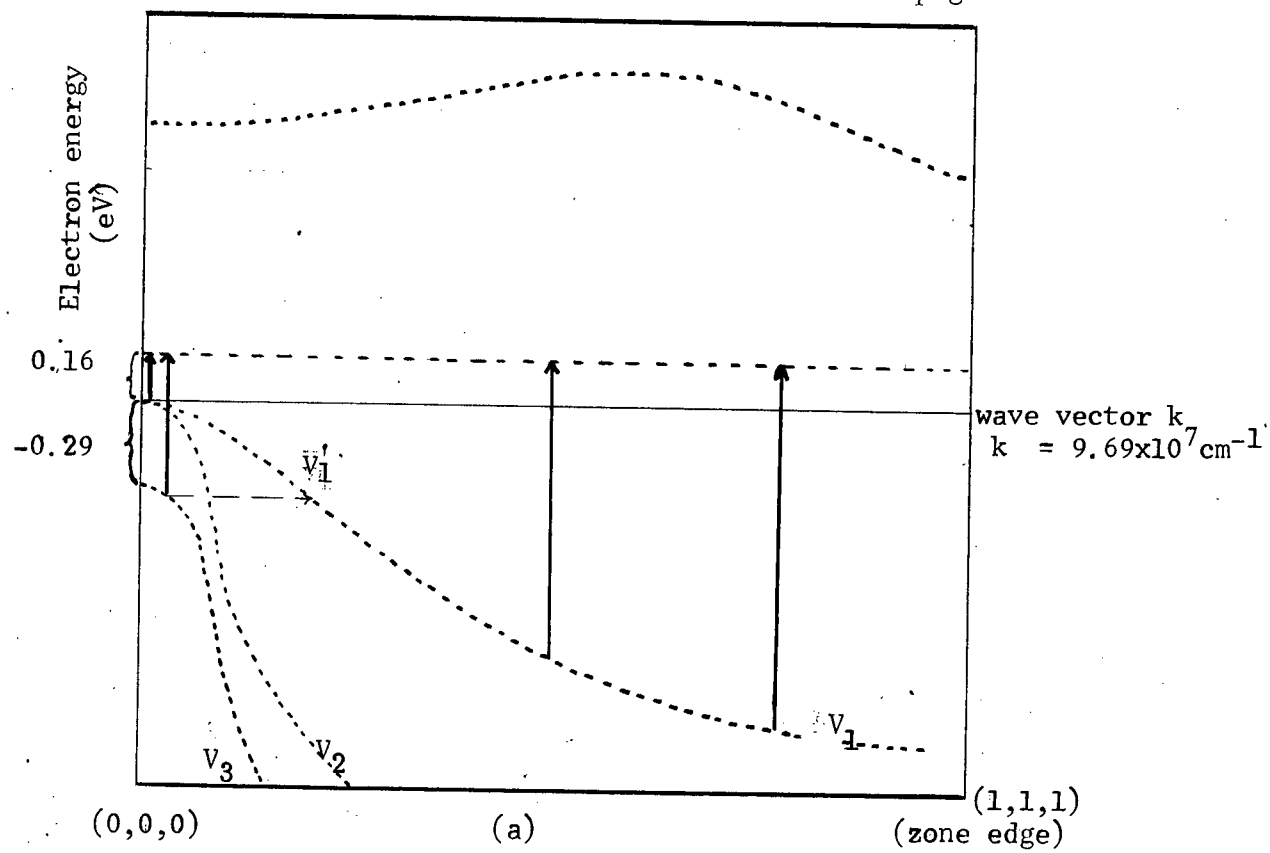

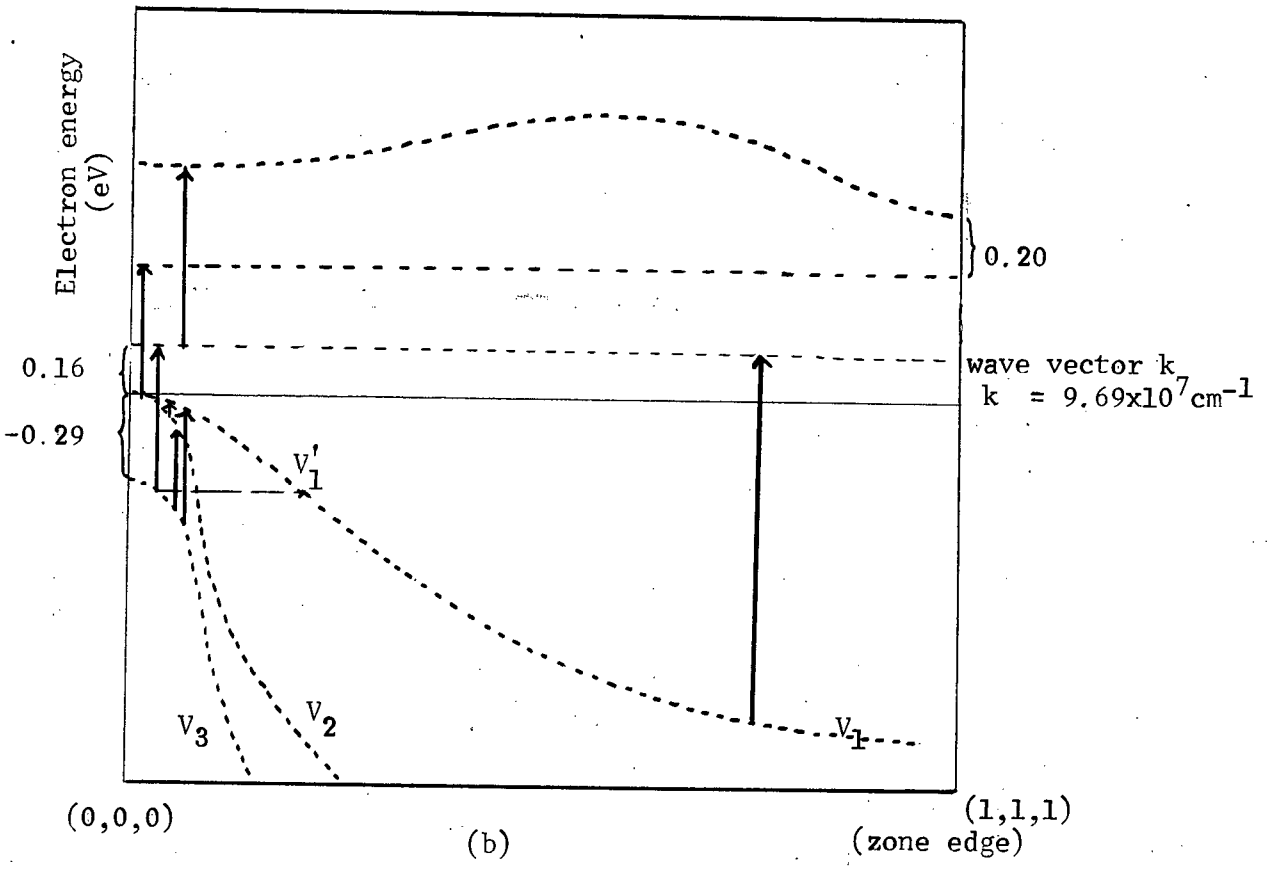

FIG 16. Graphs of energy vs k for germanium showing possible optical processes.

to follow page 40

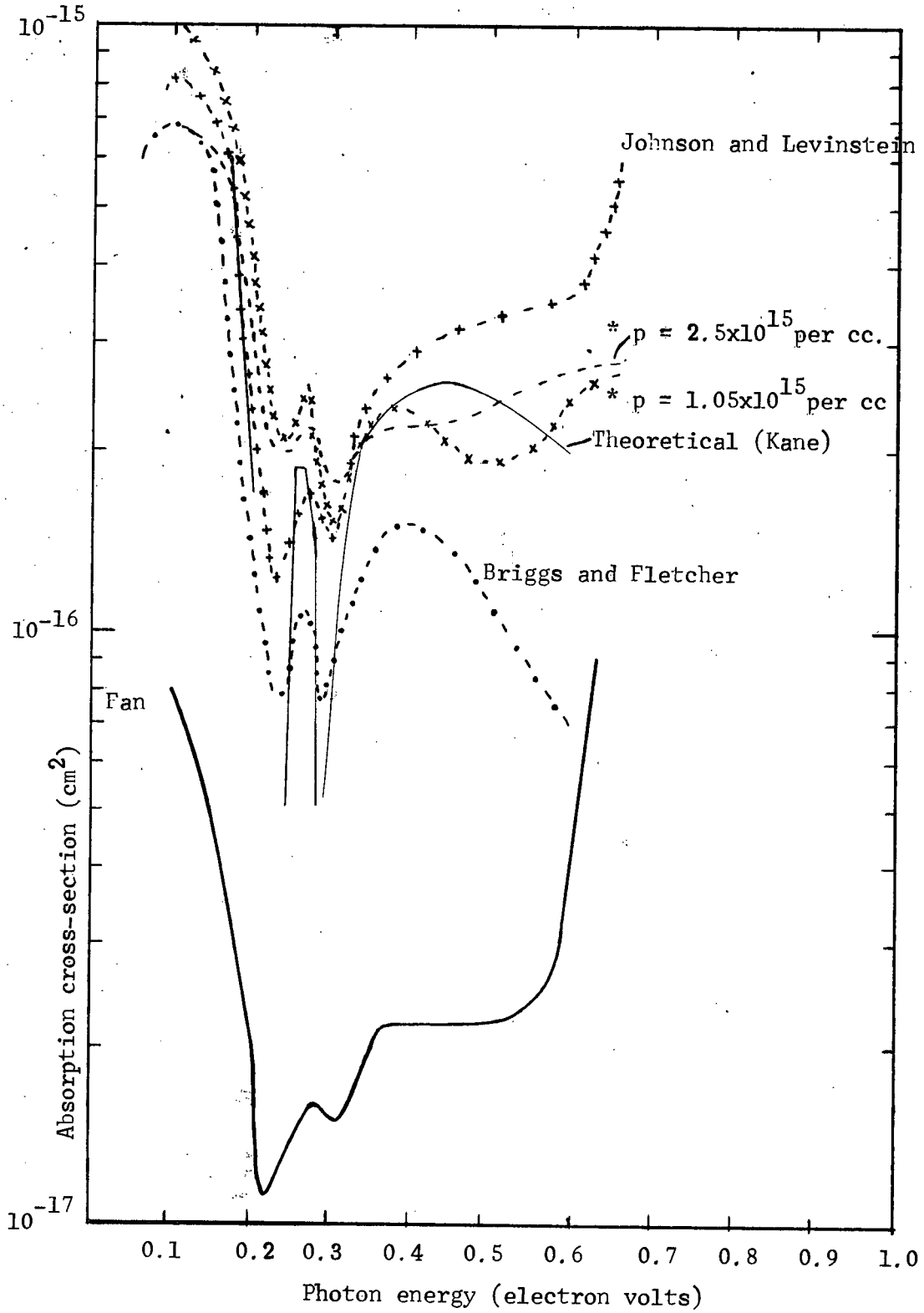

Fig 17. Absorption cross-section of germanium doped with gold and with shallow acceptors at 298 K.

The absorption below 0.24 ev is attributed to the intraband transitions between V_2 and V_1 (Figure 16(b)) and we observe (Figure 17) that the magnitude of the cross-section of absorption is in close agreement with that obtained by Briggs and Fletcher. An absorption peak is observed at room temperature for a photon energy of about 0.26 ev. This is explained on the basis of transitions of holes between V_2 and V_3 (Figure 16(b)). Optical transitions between these bands are forbidden at k=0. Away from k=0, this selection rule breaks down and electric dipole transitions can occur. (Kahn, 1955).

Several overlapping bands due to the following mechanisms are proposed for the absorption above 0.3 ev:

(i) Intra-band hole transitions between V_1 and V_3

(ii) Hole transitions from 0.16 ev acceptors to valence band states which are far removed from the center of the Brillouin zone at k=0 (Johnson and Levinstein) or due to the excitation of electrons from the V_3 band to the acceptor levels (Fan 1956).

(iii) Photo-ionization transition to V_1 from the gold acceptor state 0.2 ev from the conduction band (Fan, 1956). Since this state appears when an electron occupies one of the other levels the density of the 0.2 ev state is 2.5×10^{15} per c.c. at room temperature.

The dip in the absorption curve of the specimen containing 1.05×10^{15} holes per c.c. in the valence band at $298^{\circ}K$ beginning at 0.36 ev may be attributed to the same absorption band due to intra-band hole transitions between V_3 and V_1. In Figure 17 we note that, when reduced to unit hole concentration, all the different absorption bands observed are narrower for the specimen with the lower hole concentration. Newman and Tyler (1957) reported studies of the effects of free hole concentration and total impurity concentration on the intra-band hole absorption. With increasing concentration the structure in the spectrum becomes less pronounced. Figure 12 shows the

same effect for gold-doped germanium toward the high-energy side of V_1 to V_3 transition. Newman and Tyler have shown the importance of two effects in the interpretation of impurity effects on the intra-band hole absorption in germanium; changes in Fermi level position within the valence band, and non-vertical transitions induced by charged impurity centers. Our observations are consistent with the second mechanism. Kane suggested the idea that scattering of a carrier by a charged center produces a mixing of the k states which describe the motion of the carrier. This results in a relaxation of the selection rule $\Delta k=0$. The effect on the spectrum is to tend to wash out the structure (Newman and Tyler). Our studies also indicate (Figure 12) that this effect of sharpening of absorption bands with the lowering of impurity concentration is more pronounced in gold-doped germanium (observed only at room temperature) than in equivalent lightly doped gallium-doped germanium (shown by the dashed lines for 77°K where this effect is supposed to be most pronounced (Newman and Tyler)). Newman and Tyler's report indicates that this effect appears only when the impurity concentration is higher than 5×10^{15} atoms per c.c. in gallium-doped germanium.

The intra-band hole absorption has been calculated by Kane (1956). He gave the general second order perturbation equation for the energy bands including spin-orbit coupling as a sixth order determinant and he derived the sixth order secular equation as the leading term of a perturbation expansion of two perturbations of different orders. He calculated the matrix elements for direct optical transitions between the valence bands from the cyclotron resonance constants and computed the intra-band hole absorption from the band structure calculations for four directions. The weighted average for 300°K is included in Figure 17 for comparison.

At room temperature, further rise in absorption takes place for energies above 0.5 ev. Electron transitions from the 0.16 ev level to the conduction band are also possible at this temperature (Johnson and Levinstein).

At 195°K the absorption observed as a function of photon energy is shown in Figure 11. The broad absorption band below 0.2 ev is attributed to intra-band transitions between V_2 and V_1 (Figure 16(b)). The absorption rises more sharply for the specimen containing 1.2×10^{15} gold acceptor atoms per c.c. than for the specimen containing 3.5×10^{15} gold acceptor atoms per c.c, in which case the absorption coefficient attains nearly constant values for photon energies under 0.14 ev.

The absorption begins a sharp rise for energies above 0.23 ev. As in the case at 298°K, the presence of overlapping bands is proposed for this absorption. Again the steeper rise of the absorption band due to intra-band hole transitions between V_2 and V_1 for the specimen containing fewer gold acceptor density may be understood from Kane's mechanism, namely, indirect transitions induced by fewer charged impurity centers (Newman and Tyler).

The absorption peak observed at room temperature for a photon energy of 0.26 ev (explained on the basis of transitions of holes between V_3 and V_2) disappears at lower temperatures. This is explained according to Kane's model in the following manner. It has been stated that optical transitions between these bands are forbidden at k=0 and, away from k=0, this selection rule breaks down and electric dipole transitions can occur. As the temperature is lowered the V_2 band will become depopulated away from k=0 and the associated absorption maximum disappears. Thus one would expect to find absorption bands with widths strongly dependent on temperature.

At 195°K most of the holes arising from the gold atoms are trapped at gold acceptors and vertical hole transitions from 0.16 ev acceptors to valence band states in the proximity of the center of the Brillouin zone at k=0 are also possible. The absorption due to this mechanism is obscured by that due to the intra-band hole transitions between V_2 and V_1.

In Figure 18 the amount of absorption due to intra-band transitions between V_3 and V_1 has been subtracted from the observed absorption at different temperatures, using the cross-section data of Briggs and Fletcher at those temperatures and multiplying by the valence band hole densities. At 77°K all holes arising from the gold atoms are trapped at gold acceptors thus intra-band transitions will not be observed. So the absorption at 77°K has been included untampered in Figure 18 for comparison. It is to be emphasized that the graphs are meant at best to give only a qualitative indication of the change of the mechanism of absorption process at different temperatures. This is mainly because the exact shape of the absorption band due to the intra-band transition is dependent on the hole concentration. At 195°K and 77°K, we observe that higher amounts of absorption in excess of the intra-band hole transitions are present, indicating the takeover of absorption by Johnson and Levinstein's mechanism (vertical hole transitions from the 0.16 ev acceptors to valence band states which are far removed from the center of the Brillouin zone at k=0). Again in thermal equilibrium at a sufficiently high temperature most of the holes will be at the valence band in the proximity of k=0. The holes still bound to the acceptor states will belong to sites farther away from k=0 and one would expect the threshold of absorption by Johnson and Levinstein's process to shift to correspondingly higher energies. This effect is just what is observed from the lower curves in Figure 18.

As a matter of fact, if we apply the considerations of McLean and Paige (1962), associated with the optical edge broadening in germanium, to the absorption associated with the excitation of electrons from the V_3 band to the acceptor level (Fan's (1956) mechanism), the latter is indistinguishable from the mechansim suggested by Johnson and Levinstein. This is because of the broadening due to the large probability of holes at V_3 being scattered

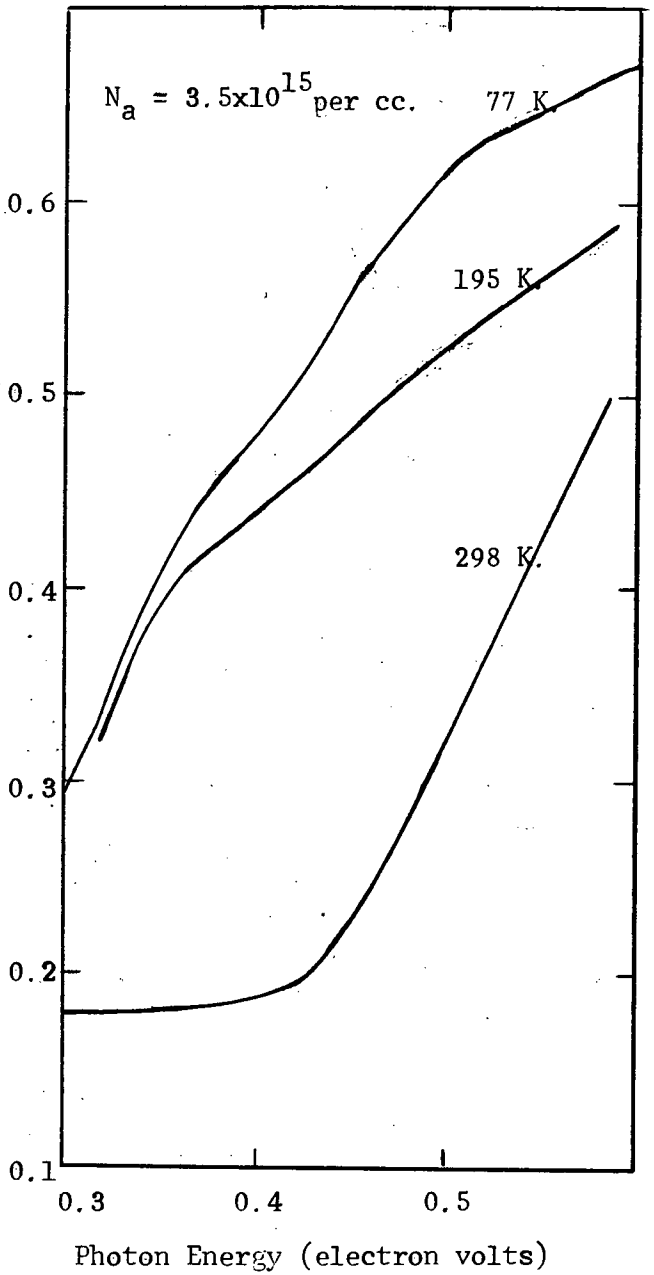

Fig 18. Absorption coefficient of gold doped (lightly doped) germanium after subtraction of Briggs and Fletcher (1952) type absorption at various temperatures.

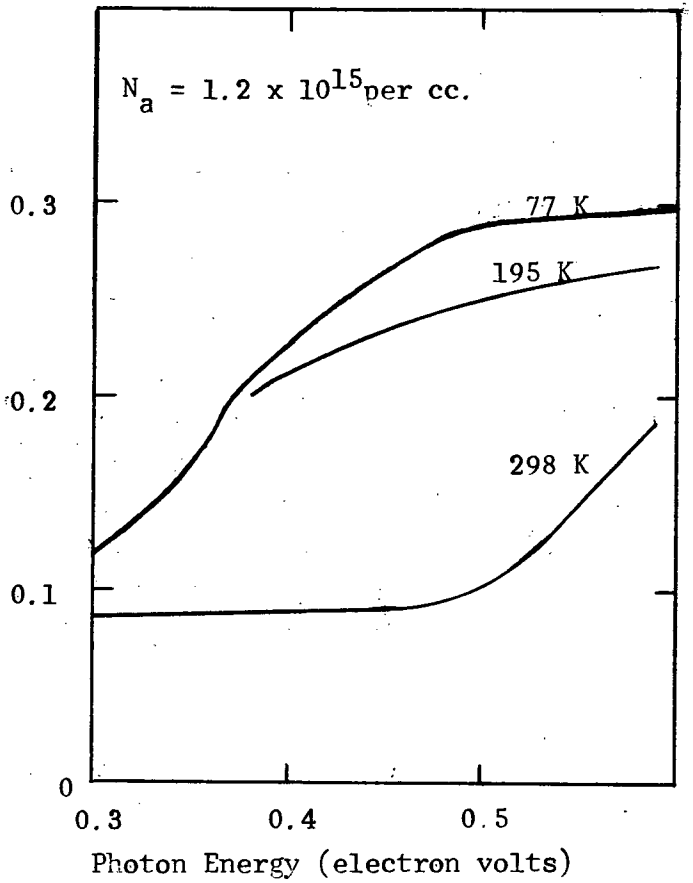

to follow page 44.

to the large density of states around V_1' (Figure 16) accompanied by the emission of almost exclusively optical photons. The deeper the level lies within a band, the broader it is at all temperatures following from a consideration of availability of final states.

6.2

Enhanced infra-red transmission through germanium at 4.2°K.

While investigating the transmitted intermediate range infra-red spectrum at 4.2°K of germanium lightly doped with gold it was noticed that the amount of transmitted light throughout the range 0.09 ev to 0.4 ev increased by about 16 per cent compared to that at 77°K.

Similar magnitudes of transmission maxima were observed recently by Hadni, Claudel, Decompes, Gerbaux and Strimer (1962) while examining absorption in arsenic-doped germanium at 4.2°K of photons having energies around 0.01 ev. Also, Macfarlane, McLean, Quarrington and Roberts (1957) stated that the infra-red transmission of all their pure germanium specimens increased by about 2% on cooling to 4.2°K between the absorption edge and 0.53 ev. They attributed this to be a lowering of the surface reflectivity rather than a significant reduction in absorption and they thought this to be consistent with Briggs' observation (1952) that the refractive index of germanium increased on heating.

It was decided to make a detailed study of this effect with pure monocrystalline germanium of different thicknesses. The resistivity of the germanium was about 50 ohm cm. at room temperature. The final polish was with levigated alumina (Linde B abrasive- on particle diameter $\sim$ 0.1 μ) on 'Selvyt' polishing cloth of medium nap. The specimens were cut from the same ingot of germanium monocrystal grown in this laboratory by the Czochralski technique.

The results of this study are illustrated in Figure 19. No significant spectral dependence of the infra-red transmission was observed in the range 0.18 to 0.30 ev, in the limit of our accuracy.

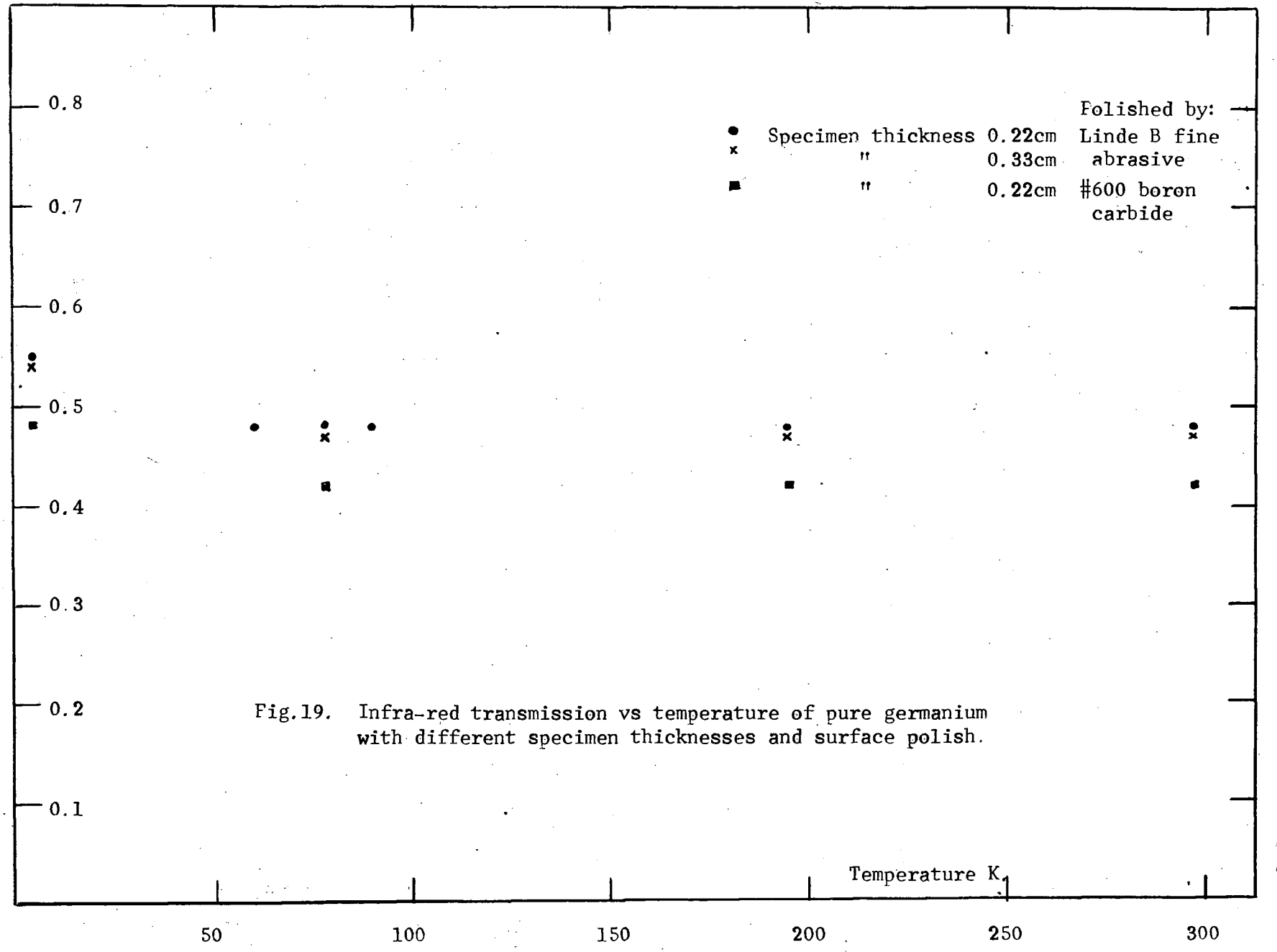

Fig.19. Infra-red transmission vs temperature of pure germanium with different specimen thicknesses and surface polish.

to follow page 45.

We attempt to explain this effect in the following discourse.

The reflectivity for normal incidence is

$$r = \frac{(\mu-1)^2 + k^2}{(\mu+1)^2 + k^2} \qquad (22)$$

(where μ is the refractive index and k the extinction coefficient), being the ratio of the intensities in the reflected and incident waves. With a good polish the reflectivity can be made to be close to the value given by this expression, corresponding to the optical constants of the crystal. Usually the extinction coefficient is small and can be neglected in (22). It follows from (22) that in the event of any change in reflectivity, there will be a corresponding change in the refractive index.

We also know that the transmission is given by

$$t = \frac{(1-r)^2 \exp(-\alpha_1 d)}{1 - r^2 \exp(-2\alpha_1 d)} \qquad (18)$$

when $\alpha = 0$, thetransmission is given by

$$t_0 = \frac{1-r}{1+r} \qquad (19)$$

Substituting for r from (22) gives

$$t_0 = \frac{2\mu}{1+\mu^2} \qquad (23)$$

or $t_0\mu^2 - 2\mu + t_0 = 0$ is quadratic having roots

$$\mu = \frac{2 \pm \sqrt{4 - 4t_0^2}}{2t_0} \qquad (24)$$

Unique measurements of the refractive index of germanium above 77°K has been reported by a number of authors. Cardona, Paul and Brooks (1959) determined μ by the method of minimum deviation and from interference in a thin germanium plate cut from a monocrystal and polished. These

measurements were carried out in a temperature range between 77° and 400K and range of photon energies 0.26 ev to 0.65 ev. In addition, there are the recent measurements made by Lukes (1960), in the photon energy range of 0.26 ev to 0.68 ev and the temperature range of 100° to 540°K using the method of minimum deviation. Above works give μ changing from 3.95 to 4 between 77°K and room temperature. Substituting this value in (23) and (19) we get $t_o \sim 0.48$ and $\eta \sim 0.35$ respectively. The above value t_o is in agreement with our observations over 60°K. The value of η also coincides with the result of Lark-Horovitz and Meissner (1949).

If the increased transmission at 4.2°K represents a reduction in absorption then (18) gives 0.6 cm.$^{-1}$ for the absorption coefficient at higher temperatures using the transmission values of the 0.22 cm. thick specimen. This value of absorption coefficient then gives 0.43 as the transmission of the thicker specimen (0.33 cm.) instead of the observed 0.47. Thus we attribute the increased transmission at 4.2°K to a lowering of the surface reflectivity rather than to a significant reduction in absorption.

Having thus eliminated absorption in the bulk as a possible reason for the change in infra-red transmission, the above phenomenon was examined as a function of the surface condition in the following manner. The spectral transmission of one of the specimens (of thickness 0.22 cm.) was observed after polishing with #600 boron carbide only. The results obtained are illustrated in Figure 19. We notice that the percentage increase in infra-red transmission at 4.2°K is the same in spite of different surface polish.

The possibility of a non-reflecting coating being formed on the surface of the specimen at 4.2°K was also looked into. The specimen inside the low temperature optical cell was always kept under high vacuum (better than 5×10^{-6} mm. of mercury) using an oil diffusion pump with boiling nitrogen trap. However, it was possible that during the precooling process prior to

the transfer of liquid helium into the cryostat the double-O-ring joint at the neck of the cryostat leaked due to extreme chill. It was found that the phenomenon persisted even after overhauling the double-O-ring joint. No difference in the effect was noticed on shutting the taps to the pumps after the transfer of liquid helium. Another test was made by placing the specimen, during the precooling, behind the shield maintained at boiling nitrogen temperature, thus making it difficult to form deposits on the specimen. This also left the effect unaffected.

(19) gives for reflectivity

$$r = \frac{1-t_0}{1+t_0} \qquad (25)$$

Substituting for t_0 (=0.55) in (25) from our measurements at 4.2°K gives $r = 0.29$ and similar substitution in (24) gives

$$\mu = \begin{cases} 3.3 \\ 0.3 \end{cases} \qquad (26)$$

Only the top value need be considered since germanium is denser than air and its refractive index with respect to air must be greater than 1.

The slight difference in transmission between the two specimens of different thicknesses polished by the fine abrasive may be due to the inability to obtain an identical surface finish.

The temperature dependence of the refractive index and the dielectric constant of homopolar semi-conductors with a diamond structure was derived by Antoncik (1956) within the framework of Kramers-Heisenberg theory, from which it follows that the square power of the refractive index

$$\mu^2 = 1 + \sum_i \frac{f_i}{\nu_i^2 - \nu^2} \qquad (27)$$

Here summation is extended to all dispersion frequencies, ν_i ; ν being the light frequency in wave numbers (cm.$^{-1}$). The corresponding values f_i are on the one hand proportional to the density of the crystal ρ , and on the other hand

to the probability of transition between the corresponding energy levels. f_i can therefore be written in the form

$$f_i = \rho F_i \tag{28}$$

F_i is a number characteristic of the atom and the transition but independent of ρ, as long as ρ is not so large that the collisions among the atoms become important (Korff and Breit, 1932). By differentiating relation (27) we obtain

$$2\mu \frac{d\mu}{dT} = \sum_i \left\{ \frac{1}{\nu_i^2 - \nu^2} \frac{df_i}{dT} - \frac{2 f_i \nu_i}{(\nu_i^2 - \nu^2)^2} \frac{d\nu_i}{dT} \right\} \tag{29}$$

From (28)

$$\frac{df_i}{dT} = \rho \frac{dF_i}{dT} + F_i \frac{d\rho}{dT} \tag{30}$$

But

$$\frac{d\rho}{dT} = -\rho\gamma \tag{31}$$

where γ is the cubical coefficient of thermal expansion. Following Ramachandran's (1947) work on diamond, Antoncik assumed that the term in (30) containing the temperature dependence of the probability of transitions can be neglected.

The use of the Kramers-Heisenberg relation (27) for non-polar materials having the same crystal structure, due to the complicated energy spectrum of the valence electrons, implies a considerable simplification of the problem. Antoncik considered that the dispersion frequencies correspond in the band scheme essentially to the direct transitions of the electrons between the valence and conduction bands and that the temperature dependence of these frequencies is conditioned by the temperature dependence of the energy levels in both bands, so that (27) corresponds very well for i=1 and

$$\frac{d\nu_1}{dT} = \frac{d\nu_{E_g}}{dT} = \frac{1}{hc} \frac{dE_g}{dT} \tag{32}$$

energy gap E_g is expressed in ergs.

Although the values $\frac{d\nu_{E_g}}{dT}$ are determined by the region of the absorption curve corresponding to indirect transitions and $\frac{d\nu_1}{dT}$ in the region of direct transitions, the assumption of the equality (32) turned out to be qualitatively satisfactory upon comparison with the measurements of Macfarlane, McLean, Quarrington and Roberts (1958) showing that the variation of direct gap E_o and the indirect gap E_g with the temperature are substantially similar in shape. Thus (29) becomes

$$\frac{1}{\mu^2-1}\frac{d}{dT}(\mu^2-1) = -\left[\gamma + \frac{2\nu_1}{\nu_1^2-\nu^2}\frac{d\nu_{E_g}}{dT}\right] \qquad (33)$$

Since $\gamma \ll \frac{2\nu_1}{\nu_1^2-\nu^2}\frac{d\nu_{E_g}}{dT}$ for $T < 100^\circ K$, according to this theory $\frac{d\mu}{dT}$ in this temperature range is practically determined by the second term on the right hand side in (33).

For the dependence $\mu = f(T)$, the agreement between theory and experiments mentioned earlier is on the whole satisfactory in the temperature range above $77^\circ K$. However, neither the refractive index nor its temperature dependence had so far been determined experimentally at $4.2^\circ K$. Only in the work mentioned in the beginning with photon energies under 0.012 ev, Hadni, Claudel, Decompes, Gerbaux and Strimer observed that for pure germanium the transmission remained very high and the refractive index as a function of photon energy remained constant with lower energies of incident photons.

In the above theory the influence of the first term in (33) involving the thermal expansion coefficient is negligible. Novikova (1960) determined the thermal expansion coefficient of germanium down to $32^\circ K$ and found that at $48^\circ K$ the thermal expansion coefficient of germanium becomes zero and on further lowering of temperature it becomes negative. However, $|\gamma|$ is of the order of 10^{-7} (and lower) per degree centigrade whereas $\frac{2\nu_1}{\nu_1^2-\nu^2}\frac{d\nu_{E_g}}{dT}$ is of the order 10^{-4} below $40^\circ K$. Thus γ has little influence on the sum of the right-hand side of (33) despite the change of sign.

ν is taken to be 1.5×10^3 cm^{-1} (0.2 ev). Values of ν_1 and $\frac{d\nu_1}{dT}$ are derived from the measurements of Macfarlane, McLean, Quarrington and Roberts (1957) mentioned previously. The coefficient of thermal expansion of germanium below $32^\circ K$ was estimated in the following manner. Daniels (1962) calculated the Gruneisen factor

$$\gamma_{gr} = - \frac{d \ln \theta_D}{d \ln V} \tag{34}$$

where θ_D is the Debye temperature and V the volume per mole, to obtain a fit with the experimental data of Novikova as

$$\gamma_{gr} = \frac{\gamma V}{\chi C_v} \tag{35}$$

where χ is the compressibility and C_v the specific heat at constant volume. Daniels further obtained the limiting value of γ_{gr} as T approaches zero. Values of γ were restored from the above results using (35). Other data used are the following: C_v from the values of θ_D of Flubacher, Leadbetter and Morrison (1959), χ from the values of Fine (1955) and McSkinner (1953), and a value for V of 13.6 c.c. per mole.

The results of the above calculations show the same qualitative behaviour of $\frac{d\mu}{dT}$ as given in the calculations of Lukes (1960), (Figure 20), that is, most of the change of refractive index with temperature takes place above $60^\circ K$, and the decrease of refractive index is negligible under this temperature. Thus we see that our requirement of about sixteen per cent decrease of the refractive index between 60° and $4^\circ K$ is unaccountable from the viewpoint of the above theory.

Attempts were made to determine experimentally the refraction index of germanium at $4.2^\circ K$ using interference technique. But no fringes were obtained with a germanium plate of about 3mils. thick, cut from a monocrystal and polished, probably because the beam of light shining on the crystal was

to follow p. 51

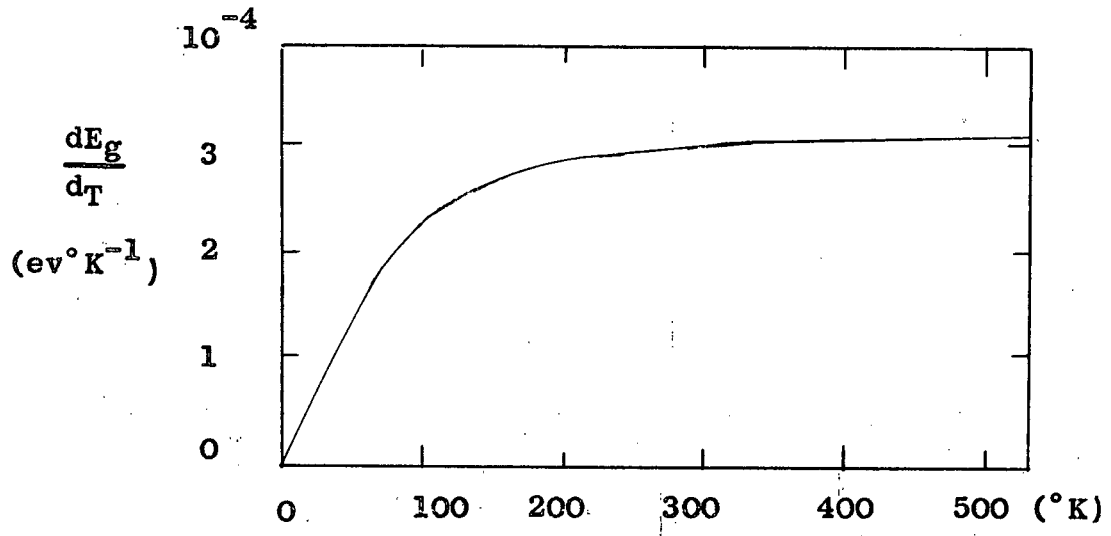

Fig. 20. Dependence of $\frac{dE_g}{d_T}$ with temperature according to results obtained by Macfarlene, McLean, Quarrington and Roberts (1957).

not parallel. However, interference fringes were obtained with about 7 μ thick germanium evaporated on mylar. But the separation of the fringes did not change between 77° and 4.2°K as required. Anyhow, that measurement should not be considered in this context as materials in the form of evaporated layers proved to have very strong minds of their own and to display properties quite different from those of the bulk material (Heavens, 1955).

The basic difficulty in the evaluation of the experimental results in the light of the dependence of the refractive index of germanium on temperature is the fact that an explicit quantum-mechanical relationship for the refractive index does not exist at present which is in harmony with the band theory of semi-conductors. Also it has been assumed in the above discourse that the term in (30) containing the temperature dependence of the probability of transitions $\frac{dF_i}{dT}$ is insignificant. This may be true as long as F_i is independent of ρ. The validity of the above assumption may be doubtful at temperatures sufficiently low such that ρ reaches a maximum and anomalous thermal expansion takes place (Korff and Breit).

6.3 Extrinsic absorption at low temperature and excited states.

Measurements of the infra-red absorption spectrum were made at 90°, 60°, 4.2°K in addition to 77°K for the specimen doped with approximately 3.5×10^{15} gold acceptor atoms per c.c. from 0.6 ev down to 0.09 ev. Determination of surface reflectivity r at 4.2°K of pure and gold-doped germanium was made by observing the transmission in the transparent region of the spectra. Under these conditions $\exp(-\alpha d) \sim 1$, and r was calculated using (19), giving 0.29 ± 0.02. Within experimental error the reflectivity remained constant at 4.2°K over the region of incident photon energies under study (0.09 ev to 0.6 ev). The value 0.29 was used for the measurements at 4.2°K.

Within experimental error, the extrinsic absorption at the above temperatures were identical. No excitation lines were seen for the Au° state in the germanium crystal.

The broadening of absorption lines has been treated theoretically (Lax and Burstein, 1955) on the basis of the scattering of the bound hole by the acoustical vibration of the lattice. The basic physical assumption made in that paper is that the broadening of the impurity levels is produced by the lattice vibrations through the electron-lattice interaction. Using the Born-Oppenheimer viewpoint, they say that the energy of a trapped hole is a function of the nuclear co-ordinates. The energy difference between a ground and excited impurity state depend on the nuclear configuration. The frequency of the absorbed radiation will then vary as the nuclei oscillate, thus leading to a broadening of the absorption. Thus at absolute zero there will be a zero-point width associated with the zero-point oscillations of the lattice. The theory indicates that the modes of importance have wave-lengths of the order of the Bohr radius of the trapped carrier state. According to this treatment, which used the hydrogen approximation for the impurity, the width is determined mainly by the broadening of the ground state and the r.m.s width of the line at $0^{\circ}K$ is expected to be of the order of the reciprocal of the Bohr radius squared. The orbit of the hole in the ground state may be sufficiently small for gold in germanium as indicated on page 39 that a major fraction of the carrier wave function will lie within one lattice spacing of the impurity atom. As the broadening of the ground state increases with decreasing orbit dimension, the failure to observe the excitation of Au° might be caused by large broadening even at $4.2^{\circ}K$.

6.4

Infra-red absorption in germanium heavily doped with gold.

Figures 13 and 14 show the absorption in heavily doped specimens containing over 10^{16} per c.c. of gold acceptor atoms at 4.2^{o}, 77^{o}, 195^{o} and 298^{o}K.

In Figure 15 the absorption coefficient α for the specimen containing 2.6×10^{16} and 1.7×10^{16} gold acceptors per c.c. has been divided by the acceptor concentrations to obtain a cross-section. Near the band gap of germanium the cross-section of absorption at 77^{o}K is nearly the same as in the case of lightly doped specimens (concentration of the order of 10^{15} gold acceptor atoms per c.c.). But while in the case of lightly doped specimens the cross-section of absorption drops sharply as energy of the incident photon decreases towards the energy corresponding to the first ionization of the gold acceptor center, the cross-section of absorption for the heavily doped specimen remains very high. At 0.16 ev, the energy corresponding to the first ionization of the gold acceptor center, the cross-sections of absorption for the heavily doped specimens are 7×10^{-15} and 1.7×10^{-16} cm^2., whereas for the lightly doped specimens the cross-section shrink to negligible values. Measurements of optical absorption in the same range were made for the heavily doped specimens at 4.2^{o}K and the observed absorption was no different from that observed at 77^{o}K.

Checks made between photon energies of 0.032 ev and 0.044 ev incident on heavily doped specimens showed that the absorption remained substantially the same at the corresponding temperatures as for the higher incident photon energies.

The curves in Figure 21 show the excess absorption in the heavily doped specimens plotted as a function of the incident photon energy. The magnitude of the excess absorption at 77^{o}K was obtained, for example, by multiplying by 2.6×10^{16} the absorption cross-section for the lightly doped specimen (containing 3.5×10^{15} gold acceptor atoms per c.c.) and subtracting

to follow p. 54

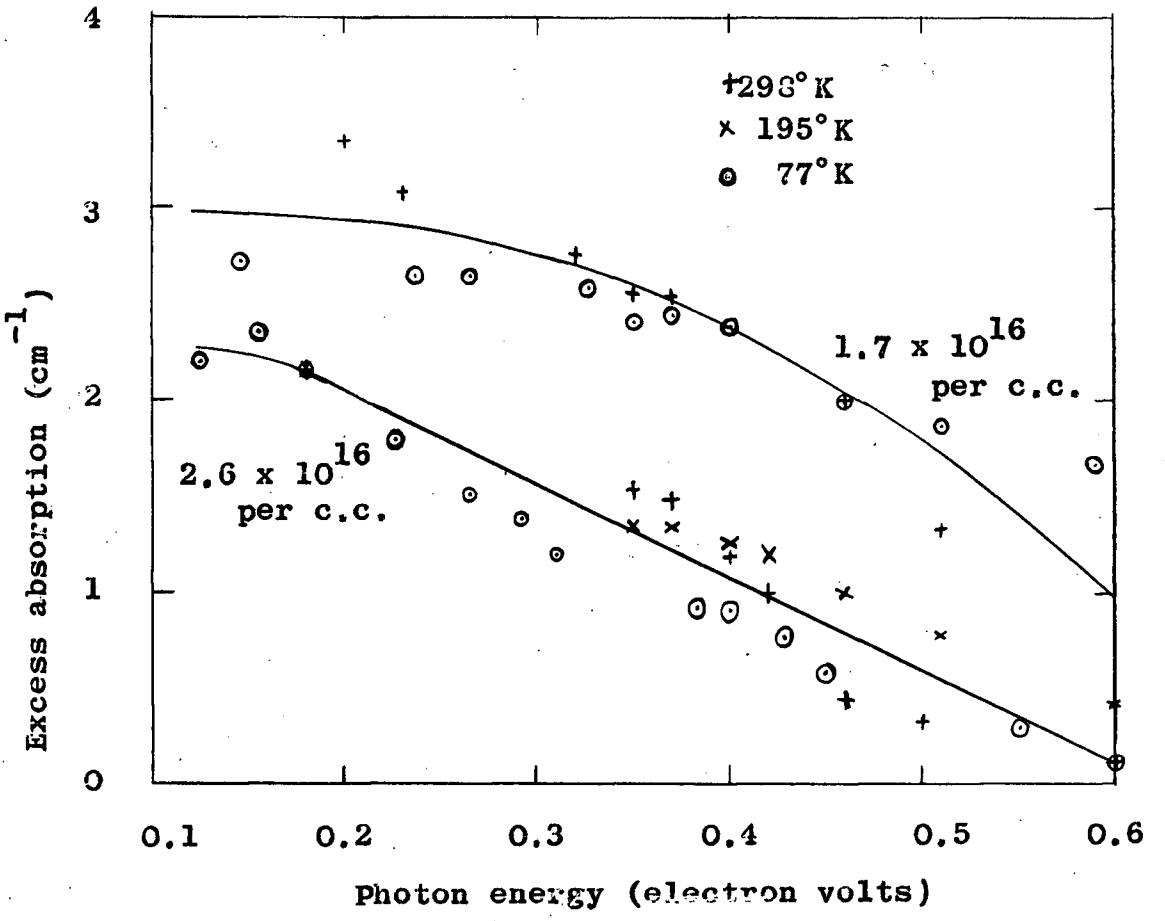

Fig. 21

Excess absorption at various temperatures vs. photon energy for gold-doped (heavily doped) germanium with different gold concentrations.

this figure from the observed absorption coefficient at 77°K for the specimen containing 2.6 x 10^{16} gold acceptor atoms per c.c. at the same incident photon energy. This may be expressed as

$$\alpha_{\text{excess at } 77^\circ K} = \alpha_{(2.6\times10^{16})} - 2.6\times10^{16} \times \sigma_{Au(3.5\times10^{15})}$$

where $\sigma_{Au(3.5\times10^{15})}$ is the absorption cross-section for the lightly doped specimen containing 3.5 x 10^{15} gold acceptor atoms per c.c.

At a higher temperature T (when intra-band absorption is present) the total expected absorption may be regarded as a sum of the intra-band hole absorption and absorption by holes at gold acceptor centers,

$$\alpha = \alpha_{\text{intra-band}} + \alpha_{Au} \qquad (36)$$

To obtain α_{Au} we first peel off the intra-band absorption from the absorption coefficients for the lightly doped specimen (containing, say, 3.5 x 10^{15} gold acceptors per c.c.) using the method described in page 44 , that is,

$$\alpha_{T(3.5\times10^{15})} - p'\sigma_{T(BF)} = \alpha_0 \text{ (say)}$$

p' being the hole density and $\sigma_{T(BF)}$ being the cross-section of absorption due to intra-band transitions at a temperature T as given by Briggs and Fletcher. For room temperature data this procedure is carried out in the region above 0.4 ev and the resulting curve is extrapolated to zero absorption at 0.16 ev. We then obtain an absorption cross-section (σ) for this by dividing α_0 by the density of un-ionized gold acceptor atoms (N_{Au} (un-ionized)) present in the lightly doped specimen at that temperature,

$$\sigma = \frac{\alpha_0}{N_{Au\,(un\text{-}ionized)}}$$

We then multiply the σ thus obtained with density of un-ionized acceptor centers present at the particular temperature in heavily doped specimens to obtain α_{Au} expected for those specimens.

α intra-band is estimated by multiplying the Briggs and Fletcher cross-section at that temperature with the density of holes (p'') present in the valence band of the heavily doped specimen,

$$\alpha_{intra\text{-}band} = p'' \sigma_{T(DF)}$$

Thus the total expected absorption for the heavily doped specimens described in the sum of (36) is obtained. The figure thus obtained at the different photon energies is subtracted from the observed absorption at corresponding energies in the heavily doped specimens to get the excess absorption at a temperature T. We recognize that the procedure outlined for the determination of excess absorption at the higher temperatures (195° and 298°K) is very crude and much credence should not be placed on the absolute values of the excess absorption. The idea is to obtain merely a qualitative picture of the temperature dependence, if any, of the excess absorption. However, no appreciable difference was found in the excess absorption for a particular incident photon energy at different temperatures.

Similar calculations for the excess absorption in the specimen containing 1.7×10^{16} gold acceptor atoms per c.c. were performed and are also plotted in Figure 21 as a function of incident photon energy.

In the previous paragraphs we have referred to the low transmission in concentrated alloys at low energies of the incident photon as excess absorption. In the following we describe how other possible reasons for this low transmission were ruled out.

Kaiser and Fan (1954) also obtained very low transmission of infra-red radiation through gold-doped germanium and they attributed this to the

precipitated gold which was stated to be clearly visible on the surface of their specimen. Careful metallographic examinations described below showed the existence of inclusions near the periphery of our crystals. Nevertheless, the particular specimens used by us both for electrical and optical measurements appeared to be single crystal and single phase. The specimens used in the present work were examined under the microscope after being etched in 3% boiling hydrogen peroxide but no precipated gold was observed in the path of the infra-red beam. Also, the surface reflectivity γ was determined by measuring the transmission of a number of specimens of different thicknesses. The observed departure of γ from 0.35 was hardly sufficient to account for the enormous decrease in transmission observed in the heavily-doped alloys.

The possibility of the excess absorption being due to the broad band of V_1 to V_2 intra-band hole transition prompted by the accidental presence of shallow acceptors is ruled out because the said band is characterized by a sharp rise in absorption under 0.16 ev whereas the excess absorption in the heavily gold-doped specimens continues unchanged in magnitude under 0.16 ev. Also the possibility of this excess absorption being due to free electrons prompted by the accidental presence of excessive shallow donors is ruled out because for free electrons the absorption varies directly with $\frac{1}{\nu^2}$ where ν is the frequency of radiation, for incident photons under 0.2 ev (Fan and Becker (1951). No such dependence is observed in this case(Fig 22). These evidences are in agreement with the electrical measurements (Part II).

We mentioned that Kaiser and Fan (1954) also obtained very low transmission of infra-red radiation through gold-doped germanium and attributed this to the precipitated gold in the specimen. In case that the gold-rich phase is existing simultaneously with germanium in the bulk of the specimen we should expect that the excess absorption to follow a dependence

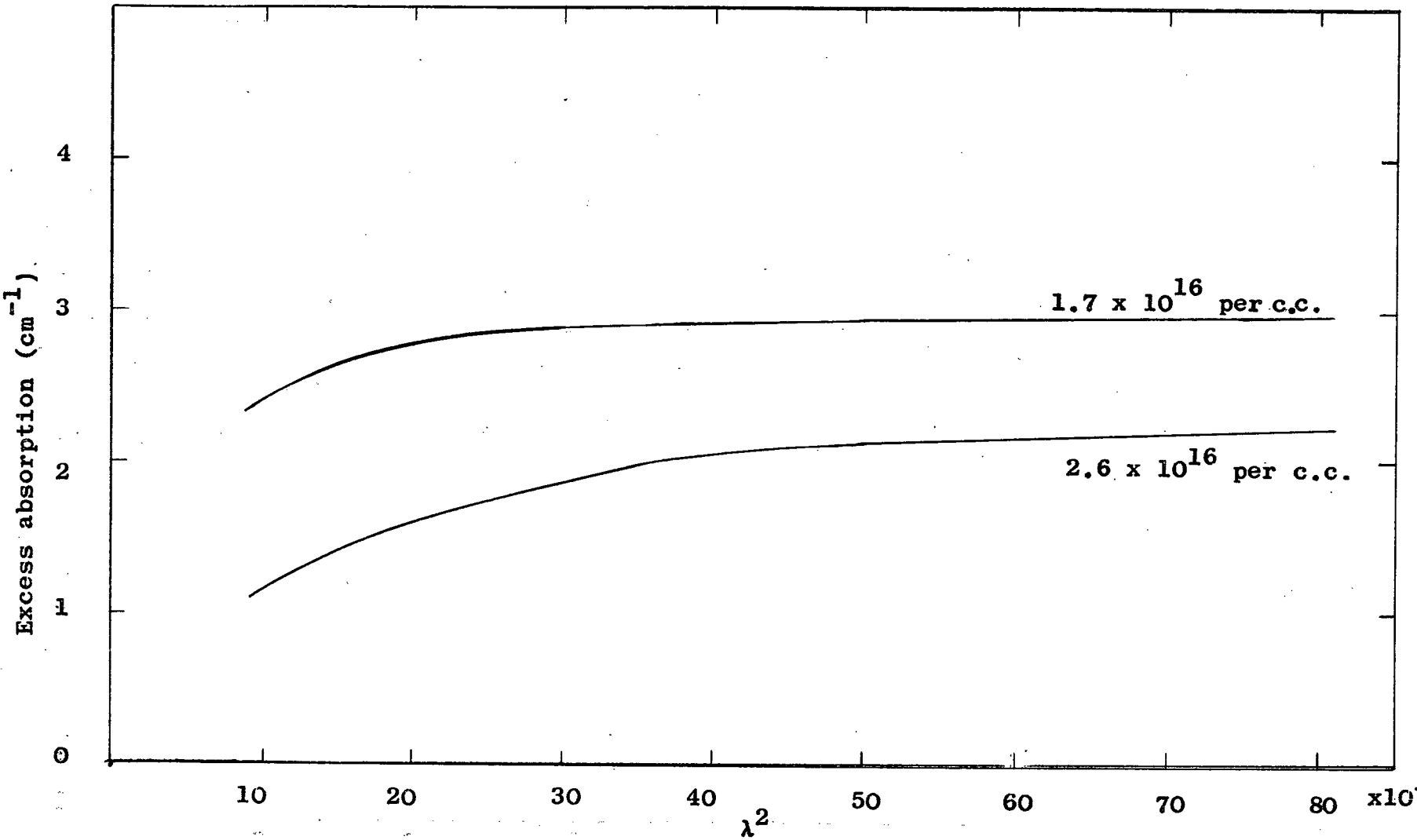

Fig. 22. Excess absorption in heavily doped specimens plotted as a function of λ^2

to follow p. 57

with incident photon energy similar to that of gold. Studies of absorption in gold by infra-red between 0.16 ev and 0.60 ev made by Hodgson (1955) show that the absorption coefficient of gold remains unchanged with the change of photon energy in this range. In our case the excess absorption changes by a factor of two within this range. Thus absorption due to the possible presence of gold crystals in the specimen may be ruled out.

It has also been suggested that dislocations may be caused by excessive impurity concentration where the solute atoms are misfits (Ellis, 1957). Furthermore, the creation of dislocations in a crystal involves the motion and mutual interaction of dislocations producing many vacancies, incipient vacancies and vacancy clusters. All such lattice debris should distort the fundamental absorption in its vicinity, and should produce an extension, a long wave-length tail, to the absorption by the crystal (Dexter, 1954). But the observations of dislocation densities in light and heavily doped specimens did not show any appreciable difference (2×10^4 to 4×10^4 per sq.cm.).

The excess absorption being an absorption band arising from localized centres in the forbidden gap bearing trapped electrons or holes was also considered. But the absence of any significant temperature dependence in the observed effect makes the above process unlikely.

Baker and Compton reported measurements of infra-red transmission observed in samples of gold-doped vapor-grown germanium. Although their measurements were inconclusive, they too showed a generally high absorption coefficient. Baker and Compton measured the solid solubility of gold in germanium grown at about 530°C below the melting point using both radio-active tracer techniques and Hall coefficient measurements. The results indicated that not all gold atoms incorporated were electrically active. Only about one atom in forty appeared to be in substitutional positions

and even the figure of 7×10^{15} atoms per c.c. reported (obtained from Hall coefficient measurements) to be the solubility in vapor-grown germanium at 405°C is far higher than to be expected ($\sim 10^{14}$ atoms per c.c.) in melt-grown germanium at that temperature. Baker and Compton suggested that electrically inactive gold may be incorporated in non-substitional positions in the lattice. Similar cases of electrically inactive arsenic in the germanium lattice has also been reported (Minden, 1960).

Our result of the lack of temperature dependence provides an important clue for the understanding of the excess absorption. The temperature independent absorption indicates that we are dealing here with a molecular stretching vibration similar to the stretching vibrations of the germanium-oxygen bond (Kaiser, Keck and Lange, 1956). The intermetallic compound tends to form at the expense of the primary solid solution when the difference in electronegativity is large. In view of the fact that a difference in the electronegativity adds stability to both the primary solid solution and the intermetallic compound, it is difficult to assign a general value to the difference in electronegativity above which extensive primary solid solution is hindered by the tendency toward compound formation. Darken and Gurry (1953) stated, however, that the difference is usually in the vicinity of one-half unit on the electronegativity scale. Electronegativity values assigned by Pauling (1960) for germanium and gold are 1.8 and 2.4 respectively, thus giving an electronegativity difference of 0.6.

It is difficult to state the form of aggregation of the excess gold atoms with germanium. Gold has been described as going into germanium substitutionally with the $6s$ electron sharing a covalent bond with one electron of the tetravalent germanium atom and thus forming triple acceptor states. Although it has been suggested in the past (Trumbore, 1960) that gold may be present interstitially in germanium, on the basis of a

theoretical treatment of solubility of interstitial impurities, Weiser (1960) considered it improbable that gold can exist as an interstitial atom to an appreciable extent. If there is more gold present than is electrically active it may be in the form of gold atoms linked to germanium with a double-bond in the following way: one 'd' electron is promoted to 6s requiring about 1.5 ev; this may be further promoted to a 6p state with a further 4.8 ev and then the gold atom is able to form a hybrid sp^3 double bond with germanium:

Au ═ Ge ═ Au

The total promotion of energy, 6.3 ev (Circular 467, U.S. Nat. Bur. Stds. (1958)) from the normal configuration of gold ($d^{10}6s^1$) is less than $4s4p^3$ promotion energy in germanium (~ 8ev , following Pauling). On the other hand, the absence of any discrete spectrum in the excess absorption makes such a definite configuration of the excess gold in germanium rather unlikely and is suggestive of perhaps a lack of any short-range order. It is also possible that four gold atoms are linked tetrahedrally with germanium with a valency of one.

Figure 21 also shows the excess absorption for the specimen containing 1.7×10^{16} gold acceptor atoms per c.c. and we see that the shape of the excess absorption remains substantially the same while the magnitude of absorption is higher. This sample was grown at about 50°C below the melting point of germanium while the specimen containing higher acceptor concentration (2.6×10^{16} per c.c.) was grown at about 33°C below the melting point. Thus the excess absorption is higher with lower temperature of growth although it has lower gold acceptor concentration. This demonstrates support to Baker and Compton's suggestion that since the incorporation of impurity is a rate process, higher than equilibrium amounts of impurity may be built-in during growth and remain frozen-in, since the growth temperature is too low for rapid atom movements to occur. These impurity atoms may form molecular

binding with nearest neighbors as discussed in the previous paragraph.

Specimens large enough for conducting optical measurements were not available from mono-crystals grown under 50°C below the melting point of pure germanium.

Part IV BIBLIOGRAPHY

Antoncik, E., (1956). Czechoslovak Journal of Physics, 6, 209.

Baker, W.E. and Compton, D.M.S., (1960). IBM Journal of Research and Development, 4, 296.

Bolling, G.F. and Tiller, W.A., (1960). "Metallurgy of Elemental and Compound Semiconductors - Proceedings of a Technical Conference, Boston", (Interscience, New York), 97.

Born, M. and Wolf, E., (1959). 'Principles of Optics', (Pergamon, London), p.40.

Briggs, H.B., (1952). Journal of the Optical Society of America, 42, 636.

Briggs, H.B. and Fletcher, R.C., (1953). Physical Review, 91, 1342.

Brooks, H., (1955). Advances in Electronics and Electron Physics, 7, 85.

Burgess, R.R., (1957). M.Sc. Thesis, Department of Physics, University of British Columbia.

Burton, J.A., (1954). Physica, 20, 845.

Burton, J.A. and Slichter, W.P., (1958). 'Transistor Technology', Vol.1, (Van Nostrand, New York), p.90.

Cardona, M., Paul, W. and Brooks, H., (1959). Physics and Chemistry of Solids, 8, 204.

Colbow, K., Bichard, J.W. and Giles, J.C., (1962). Canadian Journal of Physics, 40, 1436.

Daniels, W.B., (1962). Proceedings of the International Conference on Semiconductors, Exeter. (Institute of Physics and the Physical Society, London), 482.

Darken, L.S. and Gurry, R.W., (1953). 'Physical Chemistry of Metals', (McGraw-Hill, New York).

Dash, W.C., (1959). Journal of Applied Physics, 30, 459.

Dauphinee, T.M. and Mooser, E., (1955). Review of Scientific Instruments, 26, 660.

Dexter, D.L., (1954). 'Photoconductivity Conference, Atlantic City', (Wiley, New York), 155.

Dikhoff, J.A.M., (1960). Solid State Electronics, 1, 202.

Dunlap, W.C., (1950). Physical Review, 79, 286.

Dunlap, W.C., (1955a). Physical Review, 97, 614.

Dunlap, W.C., (1955b). Physical Review, 100, 1629.

Ellis, S.G., (1957). 'Transistors I', (Van Nostrand, New York), p.97.

Fan, H.Y., (1956). Reports of Progress in Physics, 19, 107.

Fan, H.Y. and Becker, M., (1951). Proceedings of the International Conference on Semiconductors, Reading, (Butterworths, London), 132.

Fine, M.E., (1955). Journal of Applied Physics, 24, 988.

Fisher, P. and Fan, H.Y., (1960). Physical Review Letters, 5, 195.

Flubacher, P., Leadbetter, A.G. and Morrison, J.A., (1959). Philosophical Magazine, 4, 273.

Hadni, A., Clauden, J., Decompes, E., Gerbaux, X. and Strimer, P., (1962). Comptes Rendus Academie des Sciences, 235, 1595.

Harman, T.C., Williardson, R.K. and Beer, A.C., (1954). Physical Review, 96, 1512.

Heavens, O., (1955). 'Optical Properties of Thin Solid Films', (Butterworths, London).

Hemmet, N. and MacDonald, A.L., (1961). Solid State Electronics, 3, 309.

Hodgson, J.N., (1955). Proceedings of the Physical Society of London, B 68, 593.

Holland, M.G. and Paul, W., (1962). Physical Review, 128, 43.

Johnson, L. and Levinstein, H., (1960). Physical Review, 117, 1191.

Jones, D.J.G., (1961). M.Sc. Thesis, Department of Physics, University of British Columbia.

Kahn, A.H., (1955). Physical Review, 97, 1647.

Kaiser, W. and Fan, H.Y., (1954). Physical Review, 93, 977.

Kaiser, W., Keck, P.H. and Lange, C.F., (1956). Physical Review, 101, 1264.

Kane, E.O., (1956). Physics and Chemistry of Solids, 1, 82.

Kelly, K.K., (1935). United States Bureau of Mines Bulletin, #393.

Klein, C.A. and Debye, P.P., (1960). Proceedings of the International Conference on Semiconductors (Czech. Acad. Sci.), 278.

Klein, C.A., Debye, P.P. and Ruprecht, G., (1960). Bulletin of the American Physical Society, 5, 62.

Korff, S.A. and Breit, G., (1932). Review of Modern Physics, 4, 471.

Kozlovskaya, V.M. and Rubinshtein, R.N., (1962). Soviet Physics - Solid State, 3, 2434.

Lark-Harovitz, K. and Meissner, K.W., (1949). Physical Review, 76, 1530.

Lax, B. and Mavroides, J.G., (1955). Physical Review, 100, 1650.

Lax, M. and Burstein, E., (1955). Physical Review, 100, 592.

Lukes, F., (1960). Czechoslovak Journal of Physics, 10, 742.

Macfarlane, G.G., McLean, T.P., Quarrington, J.E. and Roberts, V., (1957). Physical Review, 108, 1377.

Macfarlane, G.G., McLean, T.P., Quarrington, J.E. and Roberts, V., (1958). Proceedings of the Physical Society of London, 71, 865.

McLean, T.P. and Paige, E.G.S., (1962). Proceedings of the International Conference on Semiconductors, Exeter, (Institute of Physics and the Physical Society, London), 450.

McSkinner, H.J., (1953). Journal of Applied Physics, 24, 988.

Minden, H.T., (1960). 'Metallurgy of Elemental and Compound Semiconductors - Proceedings of a Technical Conference, Boston, (Interscience, New York), 35.

Newman, R. and Tyler, W.W., (1957). Physical Review, 105, 885.

Novikova, S.I., (1960). Soviet Physics - Solid State, 2, 37.

Oetgen, R.A., Kao Chao-Lan and Randall, H.M., (1942). Review of Scientific Instruments, 13, 515.

Pauling, L., (1960). 'The Nature of the Chemical Bond', 3rd edition, (Cornell).

Plyler, E.K. and Phelps, R.P., (1952). Journal of the Optical Society of America, 42, 432.

Ramachandran, G.N., (1947). Proceedings of the Indian Academy of Sciences, A25, 266.

Simeral, W.G., (1953). Ph.D. Thesis, Department of Physics, University of Michigan.

Smith, R.A., (1959). 'Semiconductors', (Cambridge).

Syed, A.S., (1962). Canadian Journal of Physics, 40, 286.

Thurmond, C.D. and Kowalchik, M., (1960). Bell System Technical Journal, 39, 169, (Supplement).

Thurmond, C.D. and Struthers, J.D., (1953). Journal of Physical Chemistry, 57, 831.

Trumbore, F.A., (1960). Bell System Technical Journal, 39, 205.

Tyler, W.W., (1959). Physics and Chemistry of Solids, 8, 59.

Valdes, L.B., (1954). Proceedings of the Institute of Radio Engineers, 42, 421.

Weiser, K., (1960). Physics and Chemistry of Solids, 17, 149.

Williardson, R.K., Harman, T.C. and Beer, A.C., (1954). Physical Review, 96, 1512.